NORDIC VOLCANOLOGICAL INSTITUTE 8802
UNIVERSITY OF ICELAND

ERUPTION MECHANISM AND RHEOMORPHISM DURING THE BASALTIC FISSURE ERUPTION IN BISKUPSFELL, KVERKFJÖLL, NORTH-CENTRAL ICELAND

by Ritva Karhunen

Reykjavik 1988

NORDIC VOLCANOLOGICAL INSTITUTE 8802
UNIVERSITY OF ICELAND

ERUPTION MECHANISM AND RHEOMORPHISM DURING THE BASALTIC FISSURE ERUPTION IN BISKUPSFELL, KVERKFJÖLL, NORTH-CENTRAL ICELAND

by Ritva Karhunen

Lic.Phil. dissertation in Geology

Department of Geology and Mineralogy
Åbo Akademi
FINLAND

1988

ABSTRACT

Biskupsfell eruption in Kverkfjöll, north central Iceland, took place during post-glacial time along a north-northeasterly extending fissure. The fissure is at least 8 km long; the southern part disappears under the glacier Vatnajokull. The eruption products range from hydrovolcanic ash and air-fall spatter and scoria deposits to ordinary lava flows. The total erupted volume has a minimum value of 37.5 million cubic meters. This basaltic fissure eruption shows two particularly interesting features, namely a cyclic variation in eruption mechanism and both a pronounced post-depositional welding and rheomorphism of the air-fall ejecta.

The Biskupsfell eruption occurred in three distinct phases. The initial activity phase was a hydrovolcanic one producing highly fragmented ash- and lapilli-sized tephra. The second activity phase, representing the main eruption phase was characterized by alternating Hawaiian lava fountaining and by several discrete Strombolian explosions. The eruption products consist of coarse spatter bombs and of coarse to lapilli-sized scoria. The deposits range from non-welded and agglutinated layers to partly and densely welded. Many of the densely welded units show evidence of secondary, rheomorphic flow. The third eruption phase was marked by simple upwelling of very fluid lavas through the previous explosion craters. The main controls of the intense welding of the air-fall deposits have been high discharge and high accumulation rates, which to a great extent prevented cooling of the clasts during the fire fountain events and during the deposition, respectively. The rheomorphic flowing of the densely welded deposits was then basically controlled by the high, uneven topography.

Contents

1. INTRODUCTION

During post-glacial time a powerful basaltic fissure eruption took place in the Kverkfjöll area, just north of the glacier Vatnajökull. This is called Biskupsfell eruption and the fissure is at least 8 km long, extending from the glacial border in a north-northeasterly direction. The Biskupsfell fissure produced both scoria and spatter fall deposits and ordinary lavas.

This eruption is of particular interest since the air-fall deposits show both a pronounced post-depositional welding and rheomorphism, i.e. a secondary mass flowage of the welded material. Welding and rheomorphism are common in dacitic and rhyolitic tuff deposits and ignimbrites. In basaltic pyroclasts these phenomena are rare with only a few authenticated and described examples of welded air-fall deposits. The eruption products from Biskupsfell fissure show also an interesting cyclicity in the type of ejecta produced during alternating eruptive phases.

The eruption of the Biskupsfell fissure occurred in three distinctive eruption phases. The eruption started with hydrovolcanic activity of short duration producing highly fragmented tephra deposits. The second eruption phase was characterized by alternating Hawaiian and Strombolian phases. The eruption products are composed mostly of tightly agglutinated and coarse spatter bombs and of loose, partly agglutinated coarse-grained scoria. When accumulated the still-plastic edges of the spatter bombs stuck together and formed thick beds of agglutinated spatter which

intermingle with the usually more loose scoria layers. Many of the spatter units, and some of the scoria units show a pronounced post-depositional welding. When accumulated on an uneven topography the welded deposits started to flow down the slopes and formed rheomorphic, secondary lava flows. After some time interval the third phase took place. During this eruption phase ordinary lavas were poured out from several craters along the fissure and from a couple of smaller crater rows on the side of the main fissure. No significant air-fall deposits were produced.

2. PREVIOUS INVESTIGATIONS

Welding is defined as the process of sintering together of hot vesicular fragments and glass shards (Smith 1960a; Ross & Smith 1961). The process of welding has usually been described from tuff and ignimbrite deposits of acid or peralkaline composition. In welded deposits the original form of the fragments can be unmodified, but usually the individual fragments, pumice and glass shards, have remained plastic enough to deform. A common feature is flattening of the fragments, still without changing the characteristic structure of the original fragments, but sometimes extreme flattening and slight flowage can obscure the original structure (Ross & Smith 1961). Rheomorphism ("flow change") is defined as secondary mass flowage of a welded tuff body as a coherent viscous fluid (Wolff & Wright 1981a). Like welding, rheomorphism is usually connected with acid and intermediate pyroclastic flow deposits (Cas & Wright 1987).

Welded air-fall tuffs are common in the geological record. Some of the best documented examples are the rhyolitic welded tuff in Askja, north-central Iceland and the dacitic welded tuff in Santorini, Greece (Sparks & Wright 1979). Incipient rheomorphic structures has also been noted in the Askja tuff. Further a good example of welded tuffs is the peralkaline air-fall tuff from Pantelleria, Italy; this welded tuff also shows pronounced rheomorphism (Wright 1980). One of the few documented basaltic welded air-fall deposits is the scoria eruption from Tarawera, New Zealand (Walker, Self & Wilson 1984). The Tarawera 1886 eruption and the Biskupsfell eruption in Kverkfjöll are both of particular interest because they are some of the very few authenticated examples of explosive basaltic fissure eruptions, and in both cases the air-fall ejecta shows post-depositional welding. The Tarawera 1886 eruption was a plinian fissure eruption, the Biskupsfell fissure eruption was characterized by the cyclic variation between Hawaiian and more explosive Strombolian eruption events.

3. METHODS OF STUDY

The Biskupsfell area was mapped during the summers 1986-87. The distribution, thickness and the type of ejecta were determined by detailed mapping. Detailed measurements of several sections both along the fissure and in the surrounding area were made in order to establish the stratigraphy of the deposits and to evaluate vertical and lateral changes in the sequences. Samples were collected from different layers of individual sections and from lava

flows. A preliminary map of the distribution of the lavas was drawn from the aerial photographs and details were checked in the field. In the immediate surrounding of the fissure a more detailed mapping of the ordinary lavas was made. The distribution and nature of the hydrovolcanic tephra was largely mapped by Th. Thordarson. All the photographs, unless otherwise stated, are taken by the author.

Chemical composition of the glasses from the lowermost hydrovolcanic ash and lapilli units were analyzed on an ARL-SEMQ microprobe. For getting "whole rock" analyses from the different depositional units the spatter, scoria and lava samples were melted at 1200 C in a graphite capsule in an experimental furnace for 15 minutes. The samples were then quickly cooled in water to get glass. This glass was analyzed on the ARL-SEMQ microprobe. A representative group of samples with phenocrysts was then selected for mineral analyses. The minerals are in two size groups, plagioclase phenocrysts and microphenocrysts of plagioclase, olivine and augite. In the analyses natural mineral and glass standards were used.

4. DEFINITIONS OF TERMS

4.1. Ash, scoria and spatter

In this work the following definitions and norms for the pyroclastic material are used. Size classification of volcanic fragmental material according to Fisher (1961a) is:

ash, clast size	< 2 mm
lapilli	2 - 64 mm
bombs or blocks	> 64 mm.

Hydrovolcanic ash is the general name for ejecta produced during an explosive eruption caused by the interaction of magma and water (Cas & Wright 1987). The pyroclasts consist of glassy, angular and broken-up fragments of ash and fine-grained lapilli.

Scoria refers to vesiculated fragments of basaltic magma produced during explosive eruptions (Wright, Smith & Self 1980). Scoria fragments can be modified during their flight from the vent but usually they are solidified when hitting the ground. They range from small lapilli-sized clasts up to 1 meter in diameter. The larger fragments tend to have a ropy or a bread-crust surface texture. Spatter applies to bombs that are formed from almost completely molten material (Fisher & Schmincke 1984). When hitting the surface the coherent lumps of magma are still so hot and plastic that the edges of the spatter bombs stick together and form layers of agglutinated spatter.

The most common size for the scoria clasts in the Biskupsfell is medium to coarse lapilli scoria, however, scoria bombs up to about 20-25 cm in diameter are not uncommon. Near the vent big rounded scoria bombs up to half a meter can be found. In this study the deposited scoria with all the above mentioned size-ranges is simply called scoria or scoria unit. When referring to some very distinctive layer a more specialized name may be used, for

example 'fine-grained lapilli scoria'. The scoria is composed both of uneven, fragmented and vesiculated magma clasts and of regular fusiform and spindle-shaped scoria clasts. "Cored bombs" with included xenolith are relatively common, the largest bombs range up to 30-40 cm in diameter.

The spatter deposits are usually composed of spatter bombs. Large bombs, over 1 meter in diameter are commonly found in distances over 0.5 km from the craters, situated on their original accumulation site. Smaller spatters than 64 mm are seldomly found. The deposited spatter clasts are called spatter bombs and the depositional units composed of spatter bombs will be called spatter layers or spatter units. The by far most common form of the spatter bombs is an outflattened cow-dung bomb; some irregular fusiform and spindle bombs constitute a smaller portion of the spatter units.

4.2. Welding and rheomorphism

Welding involves the sintering together of hot, glassy fragments, irrespective of shape and size (Ross & Smith 1961). According to Smith (1960a) welding is "that process which promotes the union or cohesion of glassy fragments". When deposited, the still hot and plastic pyroclastic clasts stick together and usually form layers of agglutinated pyroclasts. During welding the fragments deform and flatten out plastically forming foliation parallel to the flattened and elongated fragments. This texture is known as eutaxitic texture (Ross & Smith 1961). In welded tuffs flattened,

glassy juvenile clasts forming the foliation are called fiammes (Wright, Smith & Self 1980). In welded tuffs and ignimbrites three zones are distinguished: non-welded, partially welded and densely welded zones (Cas & Wright 1987).

The features most important in controlling welding are:

1) the emplacement temperature,
2) the sheet thickness (superincumbent load),
3) the mode of eruption and its effect on the accumulation rate and on the cooling,
4) the rate of crystallization,
5) the lithic contents, and
6) the composition of the magma and the amount of volatiles in the magma, which to a considerable degree control the viscosity (Smith 1960a; Ragan & Sheridan 1972).

In the volcanological literature on welded tuffs and ignimbrites the glass viscosity and the total thickness of the deposits are widely accepted as the most important controls for welding (Ragan & Sheridan 1972; Sparks & Wright 1979). In welded tuffs the zone of most intense welding is usually somewhat below the middle of the deposit and, more rarely, on the top. In the Biskupsfell welded units the lithostatic load seem to have had little effect on welding. The causes of welding regarding Biskupsfell deposits will be discussed in more detail in the connection with the eruption products and the eruption mechanism.

Another special post-depositional feature known from welded

tuffs and ignimbrites is rheomorphism. Deposited originally on an uneven topography the densely welded units often become unstable and start to flow. This phenomenon is called rheomorphism, i.e. secondary mass flowage (Wright, Smith & Self 1980; Wolff & Wright 1981a). Rheomorphic welded tuffs are characterized by stretched fiammes forming a lineation parallel to the flow direction (Wright, Smith & Self 1980). During the flow internal structures like flow folding, imbricated fragment structures and spindle shaped structures around rotated inclusions, i.e. around lithic fragments can be formed (Schmincke & Swanson 1967; Chapin & Lowell 1979).

In this study following classification of the degree of welding for both spatter and scoria units is used:

a) Non-welded. The units are composed of loose, unconsolidated individual fragments of scoria sometimes with loose spatter bombs in between (Fig. 4.1). Spatter deposits without any welding are rare. The pyroclastic fragments are undeformed and vesicles are rounded indicating the original form of gas bubbles.

b) Agglutinated. The individual fragments are partly stuck together. The edges of the clasts are still clearly recognizable and there is no secondary deformation visible (Fig. 4.2). The vesicles in the spatter bombs are rounded or slightly ellipsoidal caused by flattening of the bombs on impact.

c) Incipiently welded. The individual fragments have been stuck together but the edges of the clasts are still partly

Fig. 4.1. Non-welded scoria with lithic fragments (arrows).

Fig. 4.2. Agglutinated spatter and scoria.

recognizable. The fragments can be slightly deformed. The vesicles have been somewhat reduced and flattened. The color is usually darker than in the non-welded equivalents.

d) Partly welded. The individual fragments are flattened out and the boundaries of the clasts are just partly recognizable. The units are usually composed of an unhomogeneous, relatively dark matrix with lighter, somewhat diffuse, elongated fragments inside the matrix indicating the original spatter and scoria clasts (Fig. 4.3). Vesicles are reduced in size, they have also become flattened and stretched. Eutaxitic texture appears along the units.

e) Densely welded. Many of the individual spatter and scoria fragments have totally been fused together. The densely welded units are characterized by very fine-grained, dark, almost glassy matrix with some lighter elongated patches (Fig. 4.4). These light patches show the preserved relics of some larger scoria or spatter clasts. Vesicles are small and few, mostly outflattened and elongated microvesicles.

Rheomorphic flows. The rheomorphic units are composed of dark, very fine-grained, almost glassy material. Flow banding is common and secondary flow structures such as folding and rotated lithic fragments are present (Fig. 4.5). Ghostlike light remnants of original spatter fragments or of a few fragments fused together appear here and there in the dark matrix. The rheomorphic flow usually causes a lineation along the unit. The lineation parallels the flow direction, and is often perpendicular to the eutaxitic foliation of the

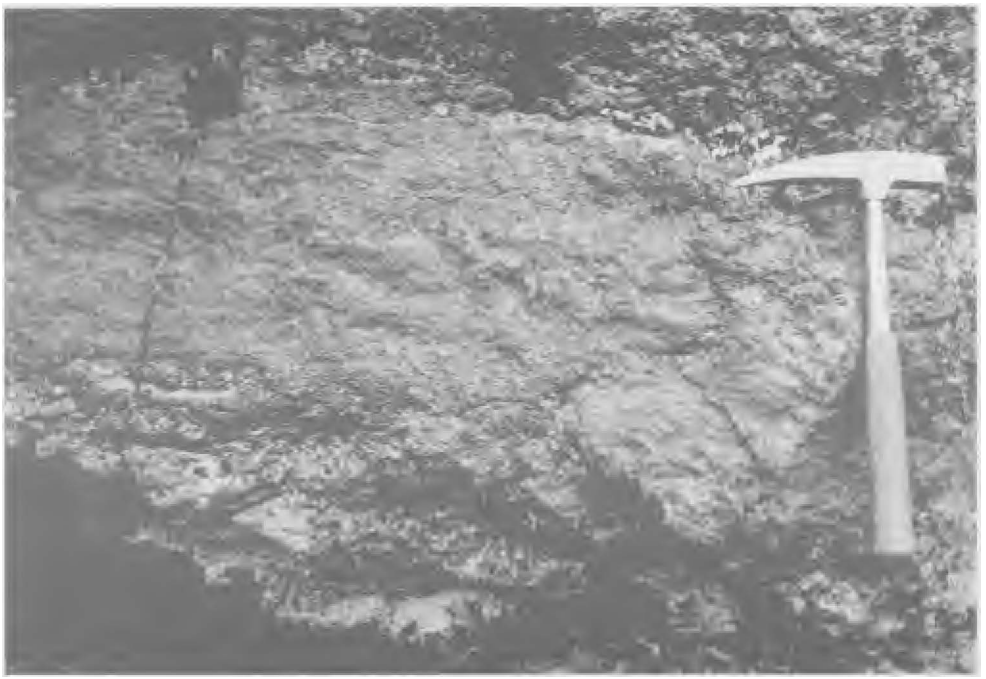

Fig. 4.3. Partly welded spatter.

Fig. 4.4. Densely welded spatter. The elongated patches (arrows) are relics of originally vesicular spatter bombs.

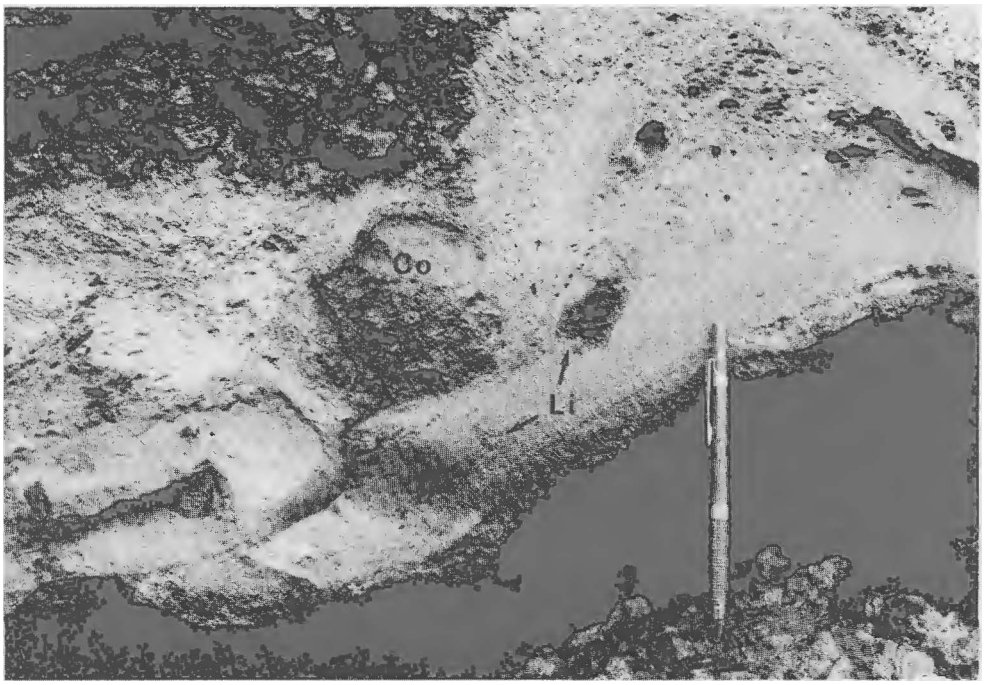

Fig. 4.5. Rheomorphic spatter flow containing cored bombs (Co) and lithics (Li).

Fig. 4.6. Rheomorphic flow, originally an air-fall spatter deposit.

welded layer. In many cases all traces of the original pyroclastic clasts disappear, and the units are very similar to ordinary lava flows (Fig. 4.6). Vesicles are highly reduced and when present appear as stretched and flattened microvesicles.

4.3. Types of eruptions and definition of units

The interaction between hot magma and water produces eruptions referred to as hydrovolcanic (Cas & Wright 1987). The water can be a groundwater reservoir or the magma can erupt directly into a body of surface water. The chilling effect of water causes rapid cooling of the magma and an explosive eruption follows. The pyroclasts produced are commonly fine-grained and angular with few vesicles. Highly viscous magmas generally form entirely glassy pyroclasts, basaltic magmas with lower viscosity tend to contain less glass and more quench crystals (Fisher & Schmincke 1984).

Hawaiian type of eruptions are characterized by highly fluid basaltic lavas of low gas content (Fisher & Schmincke 1984). They are relatively quiet effusive eruptions producing lava flows. Eruptions are often accompanied by small amounts of weak explosions when magma reaches the surface in lava fountains. The ejecta deposited from fire fountains in Hawaiian type of eruptions is usually still fluid on reaching the ground. The main ejecta consists of lapilli-sized to large bombs of spatter and in minor amounts of loose scoria. In Strombolian, more explosive type of eruptions, the ejecta consists of scoriaceous bombs, lapilli

and ash. The eruption is characterized by discrete explosions separated by periods ranging from a few seconds to several hours or days (Fisher & Schmincke 1984). In Strombolian eruptions the ejecta is, unlike in Hawaiian, nearly solid when hitting the ground, so the particles seldom flatten during deposition. Occasionally spatter bombs are formed.

Smith (1960a) classified welded ash flows that showed continuous welding as simple cooling units regardless if the unit consists of one or more flows. The flows have then been emplaced in such a close succession that they deposited and cooled virtually simultaneously. Some ash flow tuffs have several zones of welding and are then classified by Smith (1960a) as compound cooling units.

4.4. Eruption phases in Biskupsfell

The Biskupsfell eruption can be divided into three separate activity phases according to the distinctive depositional products. The initial activity phase was a hydrovolcanic one producing ash fall deposits which form a simple, unconsolidated cooling unit, the hydrovolcanic unit. The second eruption phase was the most pronounced one and also produced most of the ejected material during the whole Biskupsfell eruption event. This second phase will from now on be referred to as the main eruption phase or as the Hawaiian-Strombolian phase. During the main eruption phase spatter and scoria were ejected from several distinctive vents along the southern part of the fissure. The smallest,

individual depositional part recognized is a layer or a bed. The contacts between the different layers are often gradational, also suggesting that the ejecta was erupted simultaneously or in rapid succession from several vents. These relatively continuous depositional formations are called units.

The deposits belonging to the main eruptive phase can be roughly divided into three distinctive units. In the surrounding area west from the main fissure these three units can be found in several sections. These separate units were formed during the following eruption cycles, each marking an especially powerful and voluminous part of the eruption:

1) a Hawaiian lava fountain cycle producing mainly coarse spatter which is partly to densely welded throughout most of the sections,
2) an explosive Strombolian cycle where the major ejecta consists of non-welded to agglutinated lapilli scoria with abundant lithic fragments, and
3) a second Hawaiian fire fountaining producing spatter units which show all degrees of welding.

Along the exposed fissure walls the division of these separate cycles and distinctive units is more variable, the number of distinctive depositional units can range up to five or six. This indicates that several discrete, less voluminous eruptive events operated in rapid succession or simultaneously either in a single vent or in several vents along the fissure. Preceding the first Hawaiian lava

Fig. 4.7. Air-fall ejecta partly mantling the topography on the western rim of the Biskupsfell fissure. Note the downhill flown spatter layers (arrows).

fountain cycle smaller Strombolian explosions probably occurred. Thin, irregularly distributed lapilli scoria layers and lenses underlying the welded Hawaiian spatter unit indicate this origin. The air-fall ejecta now covers the topography except where the inclination of the underlying pillow lava ridges is very steep and the material has gravitated downslope (Fig. 4.7).

The last eruption phase, referred to as a Hawaiian lava flow phase, was marked by a simple effusion of lavas. Two clearly distinctive lavas were erupted, a porhyritic lava generated only from the southern part of the fissure and an aphyritic lava erupted through several small craters along the whole fissure.

5. GENERAL GEOLOGY OF KVERKFJÖLL AREA

Active volcanism in Iceland is restricted to three active volcanic zones. The Kverkfjöll area is located on the north-eastern volcanic zone at the northern border of the glacier Vatnajökull. The north-eastern volcanic zone is characterized by five distinct fissure swarms oriented about ten degrees northeast of north-south, each with a centrally located volcano complex (Björnsson & Einarsson 1974). Biskupsfell fissure is located inside the southernmost fissure swarm, in Kverkfjöll (Fig. 5.1). The central volcano complex is covered by the glacier Kverkjökull, a northern projection of Vatnajökull. The volcanic rocks of the northern rift zone are tholeiitic in composition, and the chemical variation observed in the eastern zone centers on the Kverkfjöll area (Sigvaldason & Steinthorsson 1974). The oldest formations in the Kverkfjöll area consist of narrow N-S to NNE-SSW trending ridges composed of subglacial pillow lavas and hyaloclastites. Post-glacial formations (younger than 10000 years) include both lava flows and pyroclastic deposits.

6. THE BISKUPSFELL FISSURE

6.1. Geological setting for the Biskupsfell fissure and the crater rows

The Biskupsfell fissure opened up through older pillow lava ridges in a NNE-SSW direction aligning the northern rift

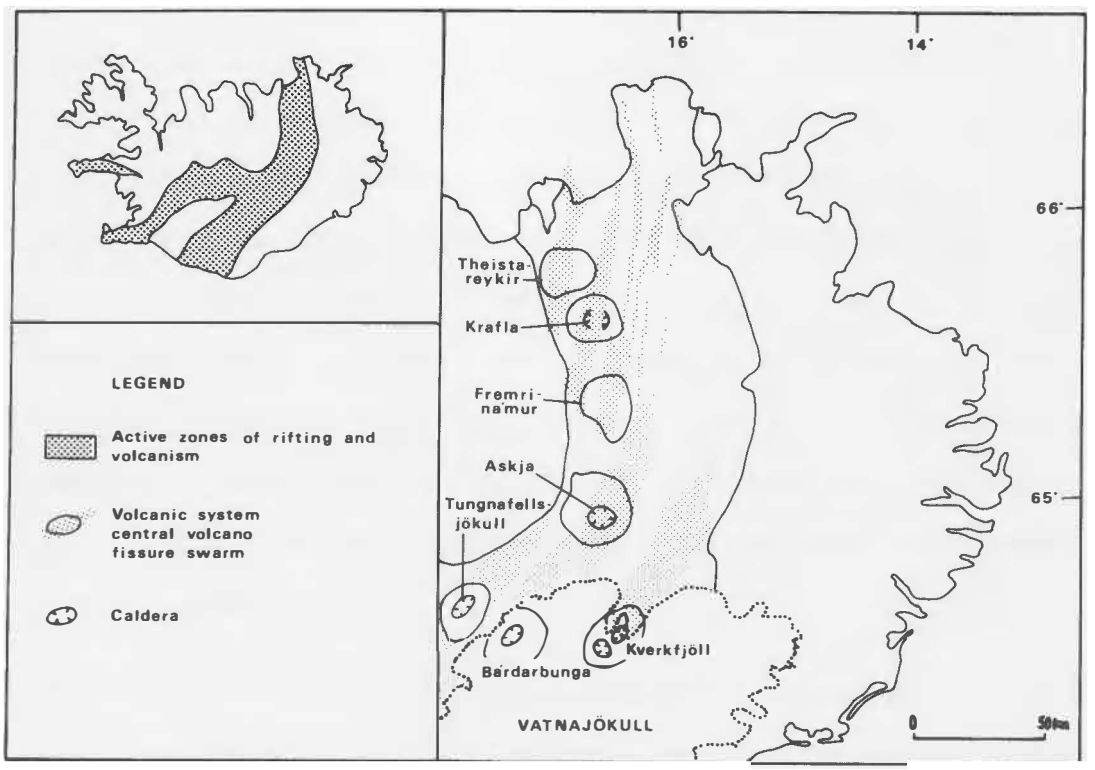

Fig. 5.1. Map showing the volcanic systems in north-eastern Iceland.

Fig. 6.1. The southern part of the Biskupsfell fissure, Eldgjá. In the foreground a shorter crater row showing the lava flow craters of the last eruption phase (thick arrows). Inside one of the craters a jeep indicates the scale (thin arrow). The glacier Vatnajokull in the background. Photo Th. Thordarson.

zone. The subaerial part of the fissure is at least 7-8 km long; it is not possible to establish the total length of the fissure because the southern part disappears below a young moraine originated from the glacier Kverkjökull. The altitude of the area is about 900 meters a.s.l. on the northern part of the fissure and rises up to 1100 meters towards the glacier rim in the south. Field evidence suggests that the main eruption took place on the southern part of the fissure, about 1.5 to 3 km NE from the present glacial margin.

There is a marked difference between the southern and the northern part of the fissure. The southern part of the fissure forms a 100 to 150 meters wide and up to 3 km long, continuous eruption fissure, Eldgjá (Fig. 6.1). This Eldgjá fissure valley will also from now on be referred to as the main fissure. On the eastern side of the main fissure there is a shorter crater row segment cutting through the northern end of a pillow lava ridge. These craters had a significant role in producing the only porphyritic material erupted during the Biskupsfell eruption. The northern part of the fissure is marked by separate, relatively short crater row segments. These craters opened up mainly on the sides of older pillow lava ridges. The northern crater rows produced just local spatter and scoria deposits, building up small cones around the craters. Short, thin lava flows pouring out through these craters marked the end of activity in these crater rows.

The early eruption was essentially hydrovolcanic. The initial eruptive vent opened up either on the southernmost

end of the main fissure, or the vent could have situated a few hundred meters to the south from the main fissure. These parts of the fissure are now covered with the glacier moraine and the initial vent area is not exposed. During this early, explosive eruption phase probably an irregular tuff cone was formed.

6.2. The eruption products

6.2.1. The hydrovolcanic unit

In the southern part of the Biskupsfell fissure layers of fine-grained, fragmented material are found under the main scoria and spatter deposits. The ejecta is mainly of two types; angular glassy shards, usually no larger than 0.5 mm, and black glassy, pumiceous lapilli, average about 0.5-1 cm in diameter. Few, small plagioclase crystals, under 0.5 mm in size, are scattered throughout this unit. The lapilli clasts are highly vesicular. The outer edges of the lapilli clasts are partly covered with short, fine-grained Pele's hair. These glassy filaments may indicate strong winds during the eruption and deposition. It is evident, that the initial activity in the Biskupsfell fissure was explosive and water was present causing a hydrovolcanic or a phreatomagmatic eruption. The fragmented lava probably erupted as quick, discrete showers of coarse ash and fine-grained lapilli forming an irregular tuff cone on the southern end of the fissure.

The hydrovolcanic ejecta contains some small xenoliths, most likely derived from the underlying bedrock during the opening of the vent. Some wind-blown fine-grained material is mixed with the original ejecta, also indicating strong winds, mixing the fine-grained surface material with the erupting tephra.

6.2.2. Scoria and spatter units

During the second, the main eruption phase, the ejecta produced shows a marked cyclicity in the type of the air-fall material. This eruption phase most probably involved the whole southern part of the Biskupsfell fissure but soon concentrated to several distinctive eruption vents. During the main eruption phase changes occurred in style of activity including alternate explosive Strombolian type eruptions and less explosive fire fountaining of the Hawaiian type. The majority of the ejecta were accumulated on the western side of the fissure (see Fig. 6.7., p. 39).

The fall deposits ejected during the Strombolian explosions consist of loose, vesicular to less vesicular, dense scoria with ragged shapes of torn lava. The clasts are mainly composed of fine- to coarse-grained lapilli. Coarser fragments include volcanic bombs, both cow-dung and ribbon bombs; some bread-crust bombs are also present. Round, regular fusiform and bipolar, spindle-shaped fusiform bombs are relatively common, ranging from a few cm to 10-15 cm in diameter. Near the vent area round fusiform bombs up to 30 cm in diameter can be found. The larger scoria bombs are

often associated with bedding sags, showing deposition from air-borne ejecta. Most of the scoria beds are non-welded or just slightly agglutinated. Partly to densely welded scoria layers can, however, be found especially in the southern part of the fissure. Situated between welded spatter thinner scoria lenses show evidence of increased welding, probably due to the heat radiation effect from the welded spatter.

During the Hawaiian fire fountaining thick layers of spatter were deposited. The spatter bombs are mainly of regular cow-dung types, the largest up to 2 meters in diameter close to the fissure. The spatter layers grade from agglutinated and incipiently welded to densely welded spatter.

Both the spatter and scoria deposits contain round "cored bombs" where lithic fragments, or seldomly just rounded scoria clasts, are coated with a layer of dense scoriaceous lava. The non-welded and agglutinated spatter and scoria deposits are usually brick-red or brown in colour, indicating oxidation during or after their deposition. Plagioclase phenocrysts, about 2-3 mm in size, occur.

There is hardly ever a complete unit composed of either scoria or spatter alone. The scoria units usually intermingle with irregular lenses composed of spatter bombs. Likewise the spatter units often consist of interlayered scoria and lenses of scoria with varying proportions. Over a distance of a hundred meter along one unit the character of ejecta can change considerably, i.e. from a spatter unit to an unit where the proportion of spatter to scoria approaches one to one.

6.2.3. Welded units

A large part of the spatter units show partial or dense welding. The welded units, including the rheomorphic flows derived from them, build up the most voluminous deposits erupted from the Biskupsfell fissure. Welding is most prominent on locations situated near the craters, however, thick units, up to 3-4 meters of partly to densely welded spatter can be found on locations situated as far as 1-2 km from the fissure. The scoria deposits are often non-welded, only along the fissure the scoria layers are incipiently or partly welded. Where welding is intense the spatter bombs form a dark grey to dark violet vitreous mass, and the boundaries of the individual spatter bombs are almost completely destroyed. Some of the original spatter bombs can be traced in form of lighter isolated patches, consisting elongated small vesicles, in the otherwise dark, massive layer (Fig. 6.2).

In the welded units lighter patches are usually composed of one to three or four spatter bombs fused together. During compaction and welding the spatter bombs have been strongly flattened forming a pronounced horizontal foliation and an eutaxitic texture along the units. Flattening and compaction increases with increased welding, i.e. the length of the original spatter bombs increases but their thickness generally decreases. The amount of flattening of the spatter grains can be used as an estimate of the degree of welding. By measuring the length/thickness ratio of the recognizable spatter grains it is possible to establish a

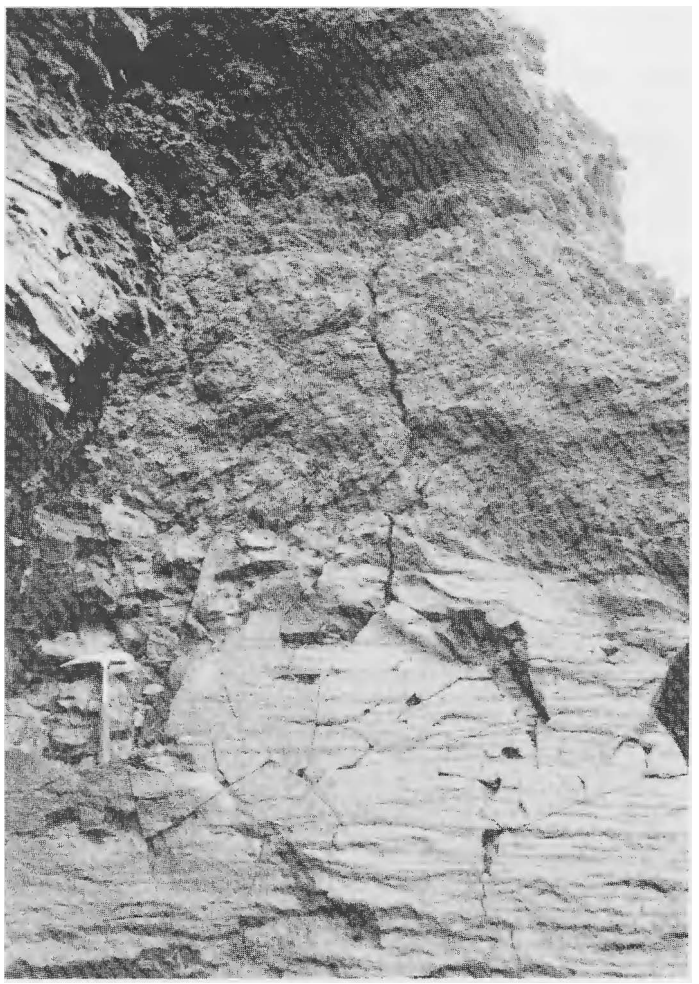

Fig. 6.2. A section situated about 1.2 km W from the main fissure showing a densely welded spatter layer passing upwards to partly welded spatter. In the densely welded layer elongated patches, representing the original spatter bombs, can be seen.

mean flattening ratio (Fr) for each welded layer. The ratios are defined from the following formula: $Fr = \Sigma Fa/n$, where Σ Fa is the apparent flatness (length/thickness) of the measured grains and n is the number grains measured. Peterson (1979) used this formula for estimating flattening and degree of welding of pumice fragments from dacitic tuffs. It is clear that the values for flattening ratios of dacitic pumice and basaltic spatter can not be compared, but the changes in flattening ratios both horizontally and vertically throughout the units gives some information of the degree of welding and can also give some indication of the relative viscosity of the ejecta during emplacement.

In estimating the Fr-ratio for Biskupsfell welded units five largest clasts in each studied section were measured. The higher the Fr-ratio the more intense is the compaction and welding. A rough estimate of the flattening ratios for the air-fall deposits was made. Flattening ratios under 4 usually indicate just a "normal flattening" of spatter bombs caused by impact. The corresponding layers range from non-welded (Fr < 2) to agglutinated (Fr 2-4) spatter and scoria. In incipiently and partly welded layers the flattening ratio ranges from 4 to 7, in these layers all the spatter bombs show some secondary deformation. Flattening ratios over 7 can be found in densely welded layers. Maximum ratios of 10 to 20 are not uncommon. In the rheomorphic layers the original spatter bombs, though visible, often have so indistinct grain boundaries that accurate measurements were not possible. Flattening ratios for different layers in two example sections are listed up in Appendix I.

In a densely welded unit the flattening ratios often show decreasing values towards the bottom and towards the top of the unit. However, in the topmost fall units, belonging to the last Hawaiian fire fountain cycle, the most intensely compacted and welded parts are situated on the very top of the layer. This phenomena eliminates the effect of lithostatic load as an important control for welding in the Biskupsfell deposits.

Small amounts plagioclase phenocrysts occur in the welded units. Due to compaction and welding the concentration of crystals per unit volume is somewhat higher in welded units than in the non-welded ones. The chemical analyses do not

show any marked differences through the welded and non-welded units erupted during the Hawaiian-Strombolian phase. This indicates that there was no chemical changes in magma composition to cause the high degree of welding in the spatter deposits.

The causes of welding will be discussed further on in the connection with the lithic contents and also in the chapter concerning the stratigraphy. The most important parameters for welding in the Biskupsfell deposits will be listed up in the connection with the eruption mechanism in chapter 8.

6.2.4. Rheomorphic flows

All the rheomorphic lavas in the Biskupsfell formation are derived from the second phase spatter and scoria deposits. The distribution of the rheomorphic flows is shown in Fig. 6.7. (p. 39). Rheomorphism is best characterized by stretched, light, ghost like patches, originally vesicular spatter bombs. These light patches usually form a marked lineation parallel to the flow direction along the foliated beds. Many of the welded rheomorphic spatter units show flow textures similar to lavas and, very intensive welding and movement of the units have created flow textures which are practically undistinguishable from ordinary lava-flow textures. However, some of these flows can be traced up to the hillsides. For these "lava flows" situated on mountain slopes no eruption fissure or vent could be found, indicating an air-fall origin for these deposits.

The necessary condition for rheomorphism of the air-fall ejecta is an original accumulation on a slope. For a welded layer to start flowing the slope need only be slight. Most of the material ejected from the Biskupsfell fissure accumulated on irregular topography which partly explains the high amount of rheomorphic spatter and also controls the distribution of the rheomorphic lavas.

6.2.5. Lava flows

During the last eruption phase highly fluid, basaltic lavas were erupted. Field evidence suggest that a series of fissure opened along the previous main fissure, and thin lava flows just poured out through several small craters. Some of the vents are marked by very low spatter and scoria cone rows. The lavas are usually small in volume, observed thicknesses of the flows seldom exceed more than a few meters. Flow distances range from a few hundred meters to 4-6 km (see Fig. 6.7., p.39).

Field evidence suggest that some time interval elapsed between the second and the third eruption phases. The contact between the rheomorphic and the ordinary lava flows is very sharp, suggesting that the rheomorphic flows had already cooled and solidified before the ordinary lavas were erupted (Fig. 6.3). Furthermore, some of the lavas flowed into a body of water or inside a snowbank. At the northern end of the main fissure there is a rounded, small gorge through which both the previous rheomorphic lavas and the ordinary lavas flowed northwards down to lower elevations.

Fig. 6.3. Contact between the II phase rheomorphic flows (on the right) and the III phase lavas (on the left). Location in the northern end of Eldgjá. In the foreground the lavas disappear down to a rounded gorge partly covered with several meters thick snow and ice layers. A hammer shows the scale (arrow).

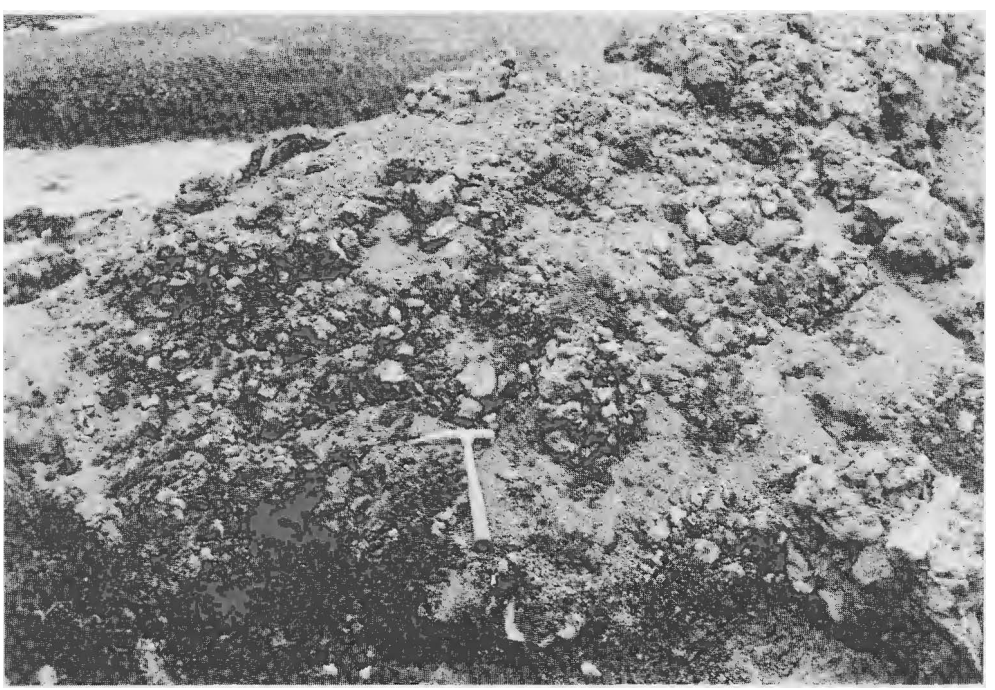

Fig. 6.4. III phase lava forming a small ridge with pillow lava-like structures on the upper surface indicating that the lava flowed inside ice or snow. Location in the northern end of Eldgjá, in a snow-covered gorge.

One of the last eruption phase lavas flown through this gorge has a form of a sharp-pointed ridge with a lower part of brecciated lava and small pillow lava-like structures characterizing the upper surface (Fig. 6.4). On the northern end of this gorge the lava ridge suddenly spreads out towards a lowland valley and forms a thin, subaerial flow with a rough, blocky surface.

The previously mentioned rounded gorge, most likely one of the central vents for the second phase explosive activity, is nowadays partly covered with snow and ice (Fig. 6.3). It is highly likely that during the time of Biskupsfell eruption the climatic conditions were relatively similar as today. The area is covered with snow and ice through most of the year, and during the summer months glacial meltwater ponds and snow covered patches are still left at the bottom of the valley deeps. Small lava flows entering this kind of water bodies or, more likely, thin lavas flowing under a hard snow cover would produce structures similar to ordinary pillow lavas. An estimate of a time interval ranging from a few years to some tens of years, enough for a snow cover to be formed, is suggested as having elapsed between the main eruption phase and the eruption of ordinary lavas.

Two different types of lavas were erupted during the last phase of activity. The first type is characterized with plagioclase phenocrysts ranging in amount about 4-5 vol.%. This lava represents the only eruption product during the whole Biskupsfell eruption with a noticeable phenocryst content. This lava erupted through several small craters situated on the eastern side of Eldgjá (Fig. 6.1., p. 18).

This porphyritic lava can be traced with certainty from the craters a distance of just half a kilometer towards north. About 2 km to the north a similar kind of porphyritic lava is exposed in a few places. It is, however, uncertain if this lava belongs to the Biskupsfell formation though its chemical composition corresponds with the Eldgjá lavas.

The porphyritic lava is mostly covered with thin, relatively rough, nearly aphyritic lavas. These lavas probably erupted in rapid succession or simultaneously through several small fissure craters situated inside the Eldgjá fissure. One of the lava flows originates from the eastern rim of Eldgjá, situated on the same line as the craters of the porphyritic lavas.

At the northern end of the Biskupsfell fissure thin lava flows were erupted through small crater row segments (Fig. 6.7., p. 39). The flows are usually no more than a few hundred meters long. They have a rough, blocky surface but are relatively thin, which indicates fluid lava of low viscosity. It is not clear if the eruption of the ordinary lavas was simultaneous throughout the whole fissure, because there is no stratigraphic contact between the southern part lavas and the lavas erupted through the crater rows situated in the north. Phenocrysts are lacking from the northern lava flows, so these lavas could correlate with the aphyritic lavas erupted from the southern end of the fissure.

6.2.6. Lithic fragments

The lithic fragments found in the Biskupsfell air-fall deposits can be divided into three categories based on their origin:

1) basement xenoliths derived from the underlying pillow lava ridges,
2) accessory lithics, found in the topmost units, consisting of fragments derived from the underlying welded units, and
3) accidental fragments having their origin in the moraine cover above and on the sides of the opening fissure.

The amount of the basement fragments is relatively low. They are made up of small, sharp-edged pillow lava fragments very similar to the pillow lava exposed on the slopes below the Biskupsfell deposits. Accessory lithics, large, densely welded fragments can be found, especially, within the second phase scoria layers. They seem to have their origin on the welded units formed during earlier cycles of the same eruption, i.e. during the first Hawaiian fire fountain cycle. A high concentration of welded fragments can also be found in some of the topmost spatter units (Fig. 6.5.). Larger lithics have often created a depression, a bomb sag, in the underlying bed, indicating that they were transported as ballistic blocks. In some of the Strombolian scoria layers dense, slab lava fragments are present. These probably had their origin in a partly consolidated crust which could have formed on the magma surface during shorter pauses in activity.

Fig. 6.5. Lithic fragments in partly welded spatter. The lithics are composed mostly of fragments of densely welded material.

Most of the lithic fragments seem to originate from the previous moraine and sedimentary cover. These lithics range in size from < 1 cm to as large as 1-1.5 m in diameter. They are often rounded which suggest emplacement from fluvial deposits. The lithics are of several types, pillow lava fragments with variable phenocryst content being most common. One type is especially rich in large plagioclase phenocrysts, this type can also be found in large amounts among the present moraine cover in the southernmost area surrounding the fissure. Lithics resembling subaerial lavas and some smaller hyaloclastite fragments are also present among the Biskupsfell deposits.

Lithics are present throughout the first and second phase units, ranging usually from 2 to 5 vol.%. The highest

concentrations are found on the western edge of the main fissure, among the second phase scoria deposits (the Strombolian cycle), varying between 5 and 10 vol.%. Lateral variation in lithic concentration is limited, horizontally the lithic-rich layers can be followed towards WSW for a few hundred meters.

Accessory and accidental lithics are derived from the previously deposited units and from parts of the moraine cover, respectively, collapsing into the fissure. The collapsing of cold lithic fragments into the magma can have a marked cooling effect on the erupting material by lowering the emplacement temperature. According to Eichelberger and Koch (1979) concentrations of 10 wt.% (ca. 5 vol.%) of cold, shallowly derived lithic fragments can easily prevent welding in air-fall tuffs. The majority of lithics in Biskupsfell deposits are from the sedimentary moraine, so they probably had a cooling effect sufficient to inhibit welding, especially in some of the Strombolian scoria deposits.

Lithic fragments are absent in the northern part of the fissure. There are two possible explanations for this feature, neither of them excludes the other. Situated further away from the glacier the moraine cover could have been missing, as well as it does at present, or the eruptions were characterized by a simple opening of the fissure craters so that no explosive vent erosion took place.

6.3. Stratigraphy of the units

The oldest rocks exposed in the Kverkfjöll are subglacially formed pillow lavas and hyaloclastites. During post-glacial time a few smaller eruptions occurred in the area before the Biskupsfell fissure eruption. In some places, located near the main fissure and in an area between 0.8-1.5 km W and NW from the Biskupsfell fissure, thick black scoria beds are found. The lowermost parts of these units consist of lapilli-sized black scoria with some coarser cow-dung bombs. The topmost part is made of partly weathered fine-grained tephra and sand, most likely formed by wind erosion of the underlying black scoria. There is a sharp break with the overlying Biskupsfell formation implying a significant time interval between these two formations. The source of the black scoria is not known.

Two smaller fissure groups are located about 1 km NNW and 2,2 km NW from the main fissure of Biskupsfell (Fig. 6.7., p. 39). These fissure groups are marked with relatively small and local scoria and spatter cone rows running in NNE-SSW direction. Field evidence suggest that these crater rows were active before the Biskupsfell eruption, the slopes of the cones disappearing under the Biskupsfell rheomorphic flows.

The Biskupsfell deposits were build up in stratigraphic order during the following eruptive phases, starting from bottom to top:

1) The hydrovolcanic phase. The initial stage of Biskupsfell eruption was an explosive interaction between surface

water and magma. The eruption products consist of glassy ash and lapilli.

2) The Hawaiian-Strombolian phase. This stage of activity marks the main phase of the eruption when also most of the material were ejected. The variation in eruption products is due to several cyclic changes in the eruption mechanism. However, three relatively distinctive, more powerful eruptive cycles can be traced up in following stratigraphic order:
   a) a Hawaiian cycle where the main ejecta consists of spatter bombs,
   b) a Strombolian cycle where the depositional units are composed of scoria with abundant lithic fragments, and
   c) a second Hawaiian cycle producing mostly spatter. Scoriaceous material was ejected in lesser amounts and some lithic fragments are present.
3) The Hawaiian lava flow phase. This last stage of the eruptive history at Biskupsfell is represented by upwelling of magma through the previous explosive craters.

The source for the hydrovolcanic ejecta was situated on the southernmost end of the Biskupsfell fissure, probably on the southern end of Eldgjá or a few hundred meters SE from it where traces of a crater row segment can be found, partly exposed amongst the moraine cover. The thickest tephra layers are situated around this southern Eldgjá area. However, the thickness and nature of the hydrovolcanic layers vary greatly suggesting that the activity occurred as a number of short explosions through several vents, either

simultaneously or in rapid succession. Field evidence suggests that a strong northeasterly wind scattered most of the ejecta towards south and southeast.

During the main eruption phase, the air-fall ejecta built up thick sections now mantling the older topography. Welded spatter deposits can be found mantling the slopes as steep as 25°. Although the main eruptive event is divided into three separate cycles it should be kept in mind that this division is somewhat simplified. Due to the cyclicity in eruption mechanism the sections are composed of several distinctive, lens-like units, some of which can be traced in the field from section to section for several hundred meters. The distribution of the individual lenses was to a high degree controlled by the force of the eruptive outblow, the topography and the prevailing winds. In many places distinctive horizontal layers intermingle with each other. Intermingling is very pronounced along the fissure walls, indicating nearly simultaneous explosive pulses through several distinct vents inside Eldgjá.

An excellent example of two welded spatter units being joined to each other as rheomorphic flows can be seen on the western rim of the fissure, shown in Fig. 6.6. This phenomena strongly implies the idea of high temperature during the eruption and rapid accumulation of the ejecta, i.e. the both layers were hot enough to weld and join together after accumulation. Between the spatter units there is a coarse-grained lapilli scoria unit which is very rich in lithic fragments. The high lithic concentration probably cooled the scoria enough to inhibit its welding.

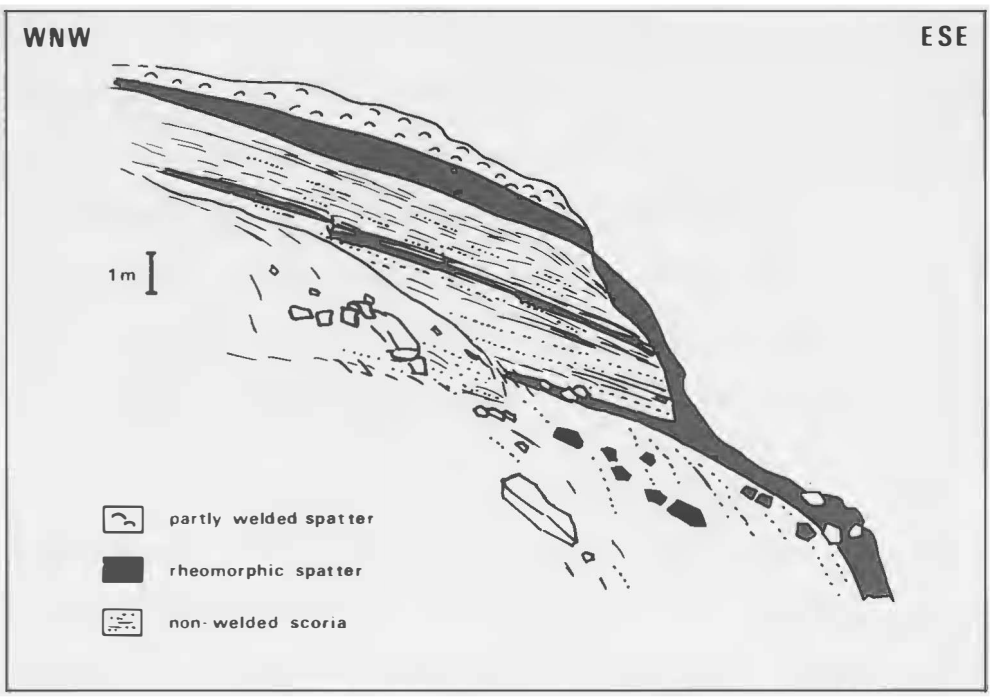

Fig. 6.6. Two welded units joined together forming a rheomorphic flow on the western rim of Eldgjá. Between the spatter units lies a thick non-welded scoria unit containing abundant lithic fragments.

The scoria and spatter deposits do not show total mantle bedding. As mentioned earlier, the topography controlled to a great deal the distribution and also the thickness of the deposits. The thicknesses of the units varies greatly, moreover, due to compaction, welding and rheomorphic flowage. Maximum thicknesses are usually found at lower elevations, in valley depressions, and where the slopes are more gentle.

On steeper slopes especially the welded units are much thinner, and on the steepest slopes the deposits are totally lacking exposing the underlying pillow lava ridges. A map showing the depositional area of the air-fall ejecta and the distribution of the rheomorphic flows is presented in Fig. 6.7.

During each eruptive pulse the ejecta was blown to west and southwest due to strong easterly and northeasterly winds. The accumulated ejecta formed elongated lateral lenses of spatter and scoria, and some of the individual layers formed during one explosive pulse can be traced in the field for about one kilometers distance from the main fissure.

Dispersal maps (Figs. 6.8-6.10) are given for each fall deposit of the main eruption phase, i.e. for the first Hawaiian cycle, for the Strombolian cycle and for the second Hawaiian cycle. Two profile maps illustrating the stratigraphy of the air-fall ejecta from a number of key locations are shown in Figs. 6.11. and 6.12., drawn parallel and perpendicular to the fissure, respectively. In Appendix I two representative sections are described in more detail.

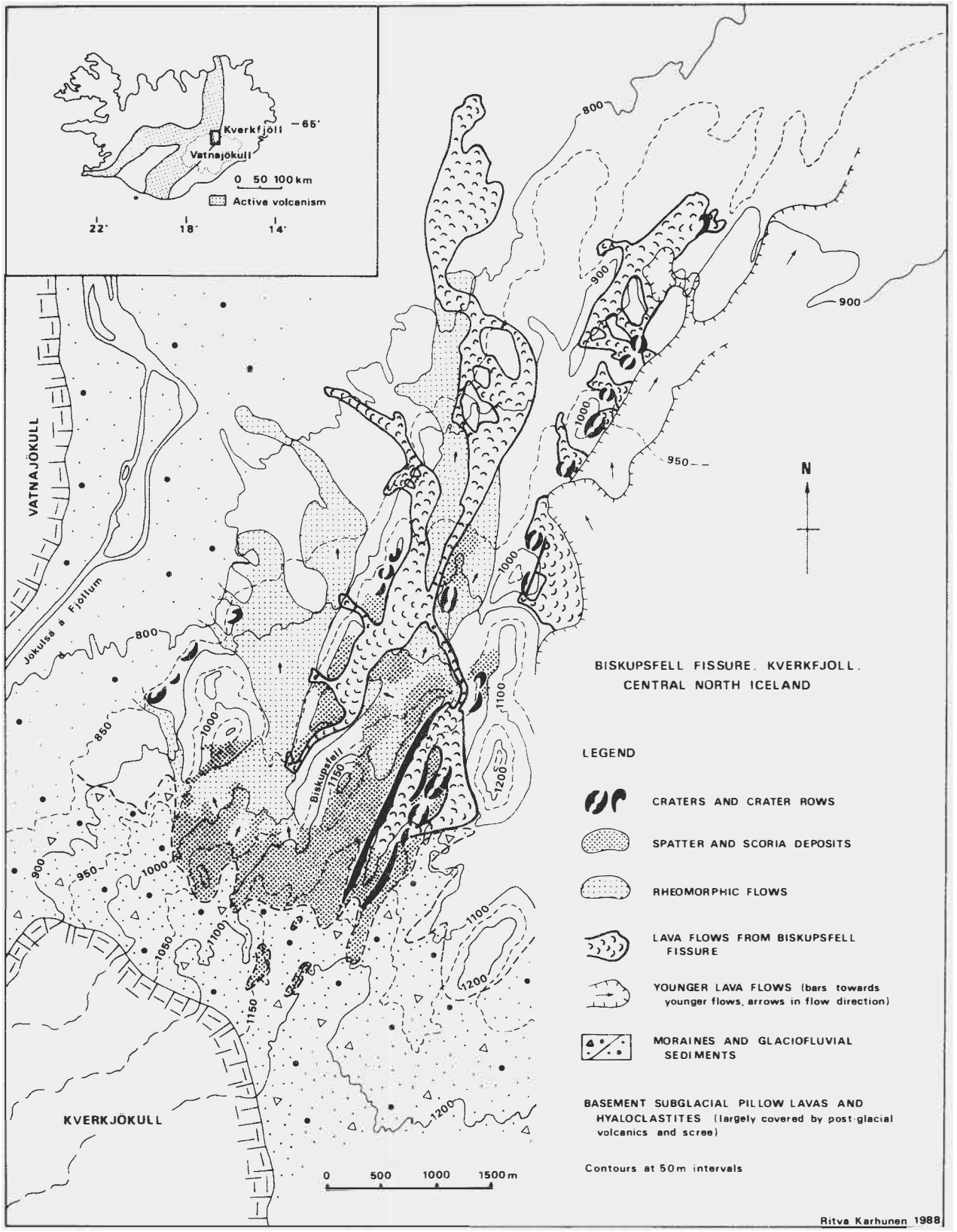

Fig. 6.7. The depositional area for the second phase air-fall ejecta and the distribution of the rheomorphic and of the ordinary lava flows (third phase).

The isograde maps (Figs. 6.8-6.10) show the thicknesses of the units (a), the average maximum diameters of the three largest spatter bombs (b), lithic fragments (c) and cored bombs (d). The thickness isogrades are drawn on the basis of the data which best gives the original thicknesses of the units, i.e. where the thickening and thinning of the unit seem to be least affected by any rolling or rheomorphic flowing. The thickness isogrades are, however, of limited value because most of the spatter units are more or less compacted and welded, but the isogrades give, however, a basic indication of the distribution of the ejecta.

The maximum spatter, lithic and cored bomb isopleths form elongated loops, partly overlapping each other, extending from the fissure to west and southwest. The lens-like appearance of the isopleth loops clearly demonstrates the cyclic nature of the eruptive events, especially concerning the Strombolian episode when explosions occurred contemporaneously or in rapid succession in different parts of the fissure. The distribution of the lithic fragments makes a good example of this phenomena. The uneven distribution of the lithics was, however, also caused by the collapsing of parts of the sedimentary covered crater walls into the erupting vents. Along the western rim of the fissure number of distinct, lithic-rich scoria lenses can be found. These lenses usually range horizontally from one hundred up to several hundred meters.

After the main Hawaiian-Strombolian eruption phase the activity in Biskupsfell fissure ceased for some time. The rheomorphic flows were already cooled down when the lavas

I HAWAIIAN CYCLE

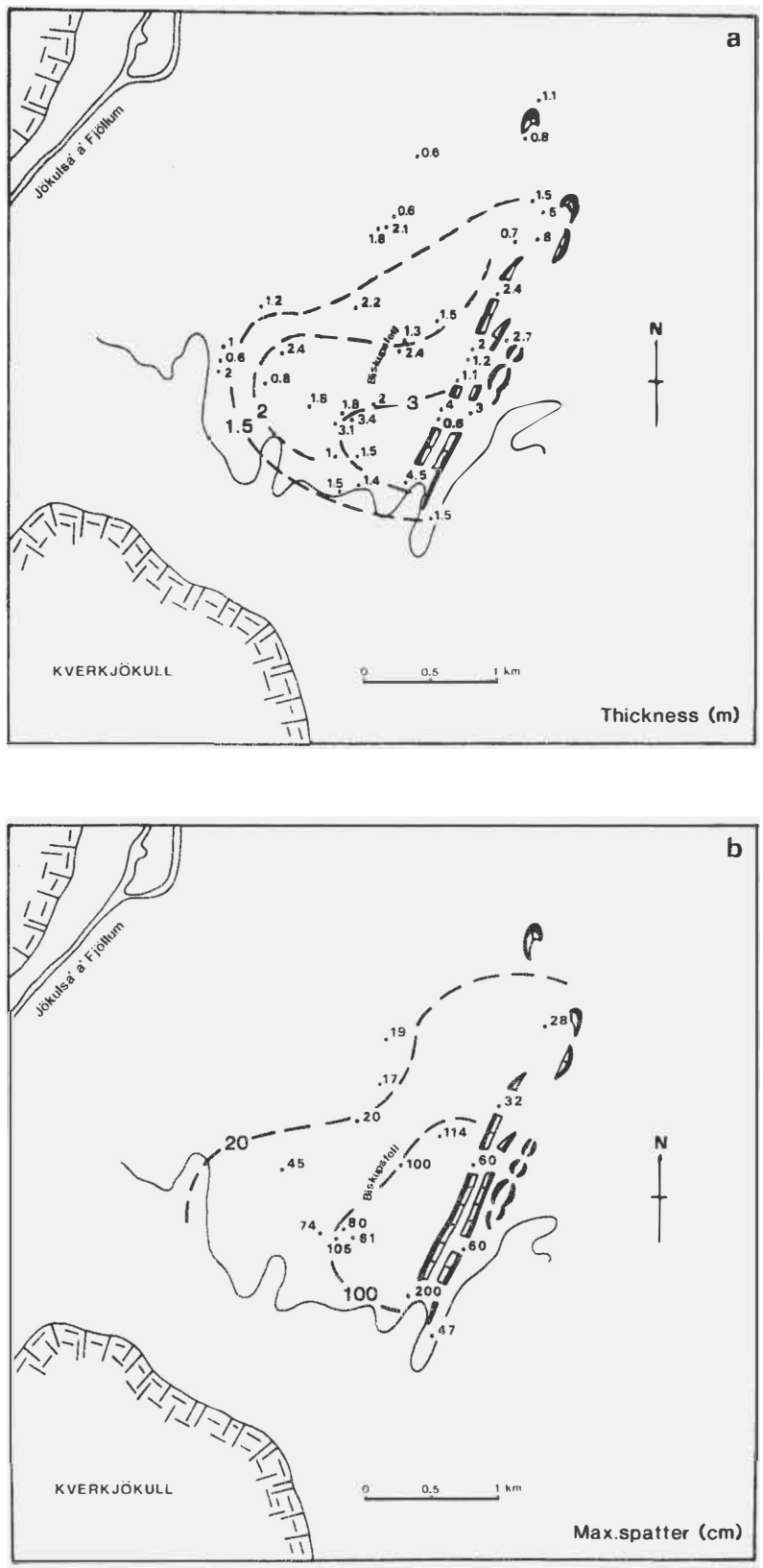

Fig. 6.8. Isograde maps for the fall deposits of the I Hawaiian eruption cycle. Three maps are given.

I HAWAIIAN CYCLE

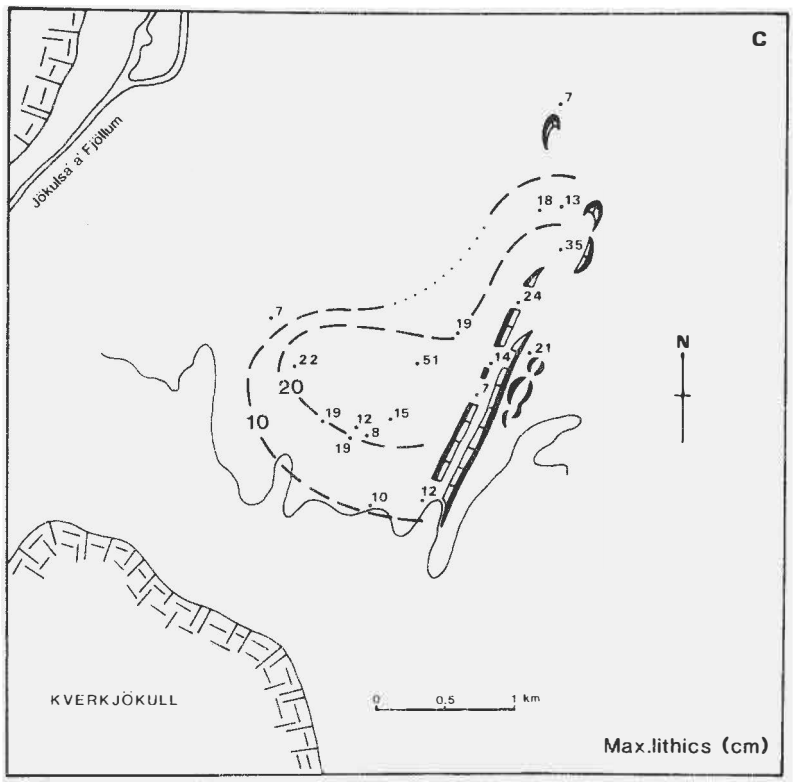

Fig. 6.8. continued

Isograde maps in Figs. 6.8-6.10:
(a) thickness, in meters,
(b) average maximum diameter of the three largest spatter bombs, in cm,
(c) average maximum diameter of the three largest lithic fragments, in cm, and
(d) average maximum diameter of the three largest cored bombs, in cm.

STROMBOLIAN CYCLE

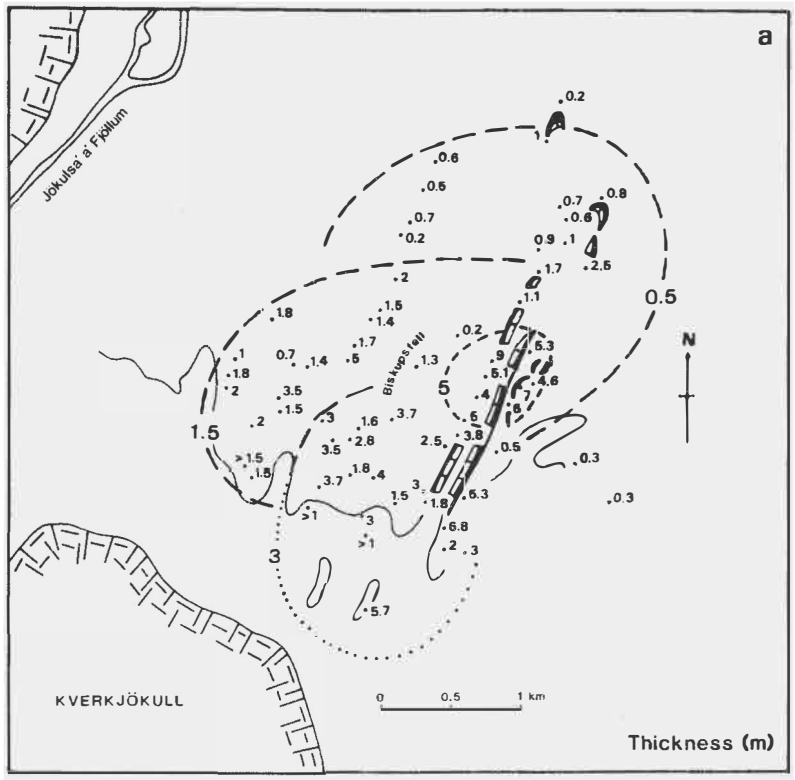

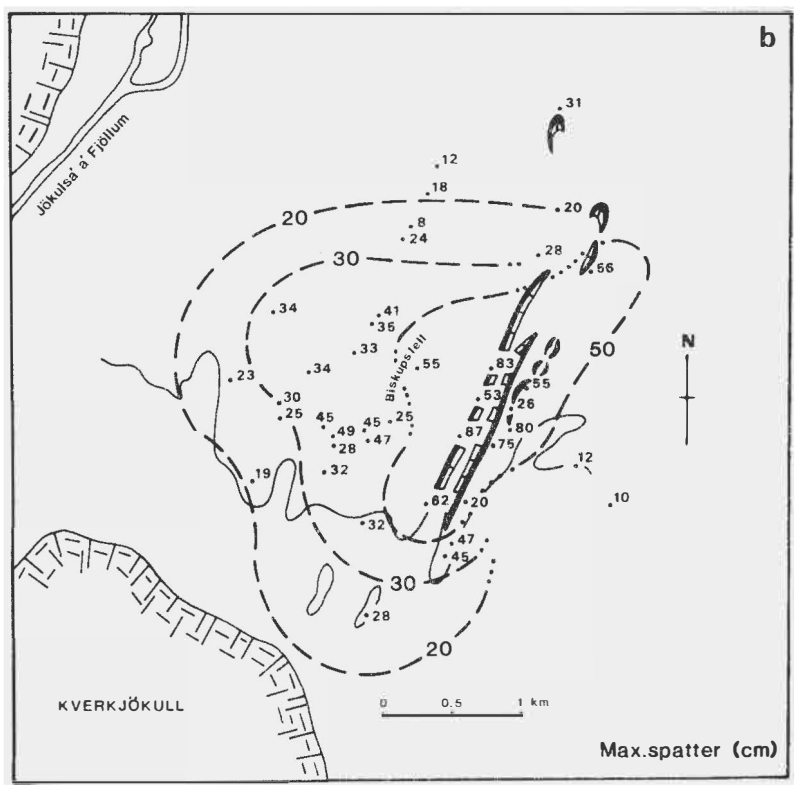

Fig. 6.9. Isograde maps for the fall deposits of the Strombolian eruption cycle. Four maps are given.

STROMBOLIAN CYCLE

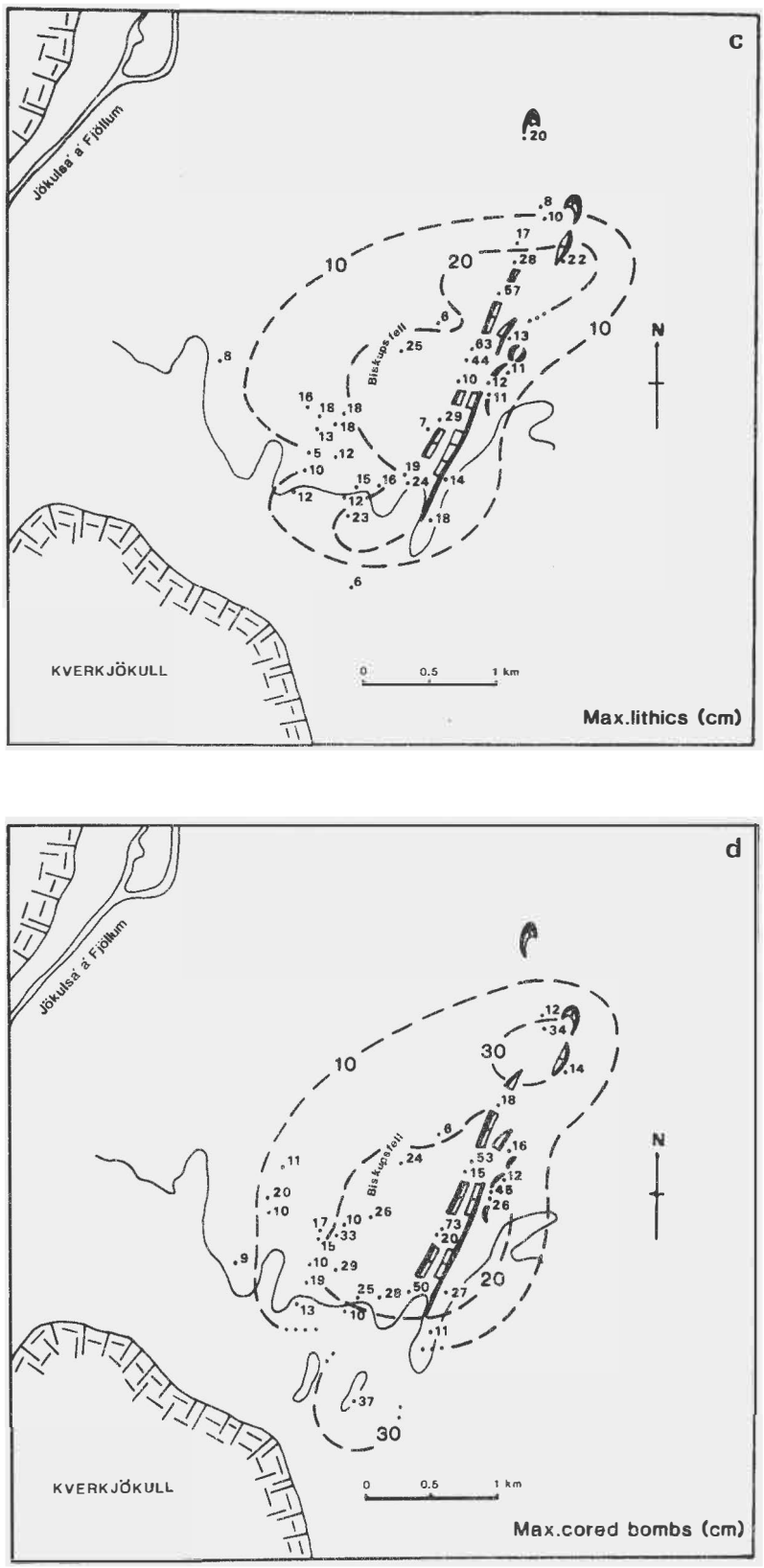

Fig. 6.9. continued

II HAWAIIAN CYCLE

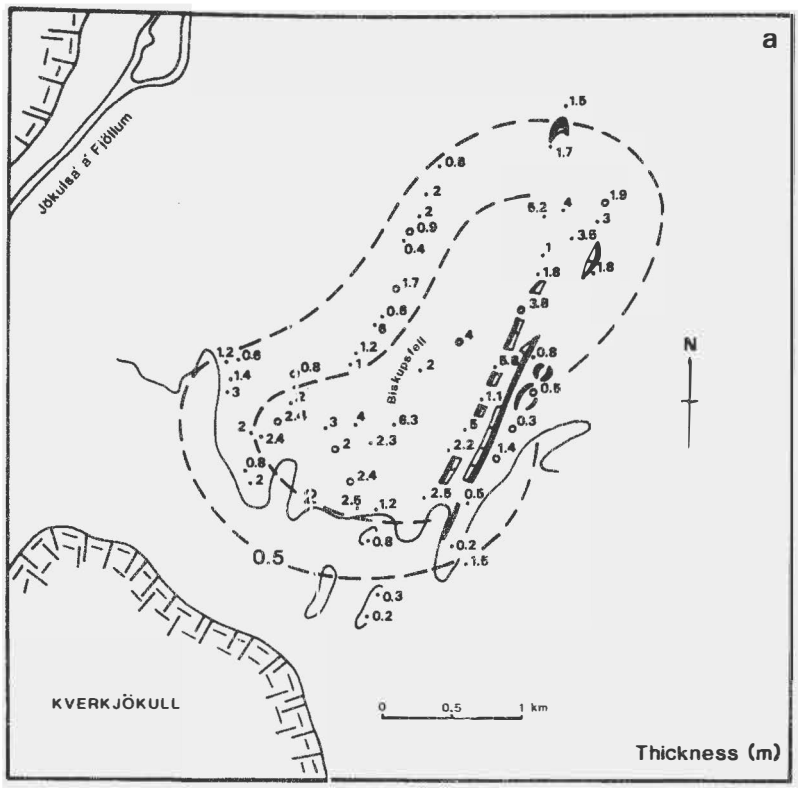

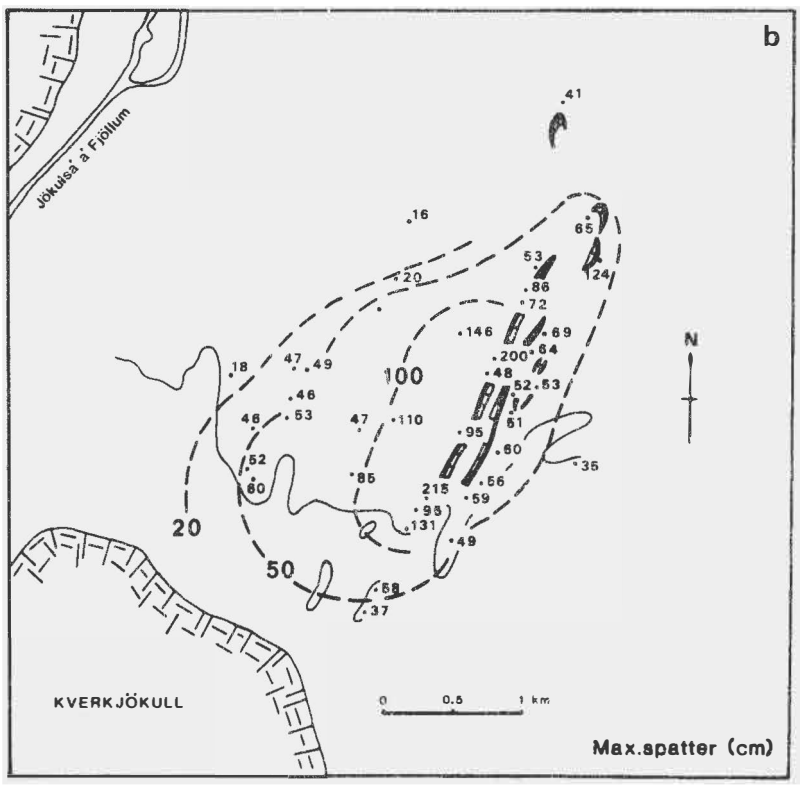

Fig. 6.10. Isograde maps for the fall deposits of the II Hawaiian eruption cycle. Four maps are given.

II HAWAIIAN CYCLE

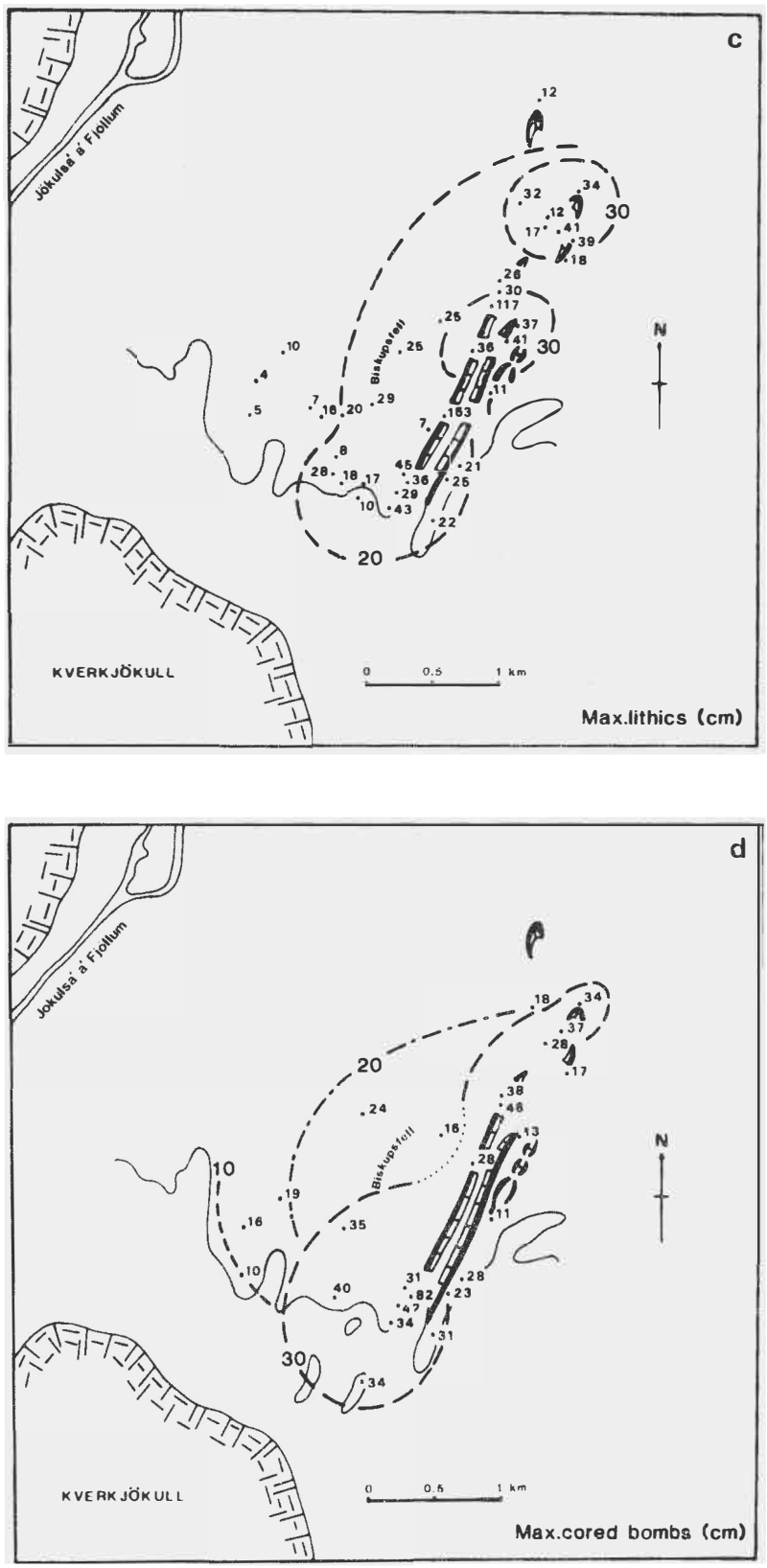

Fig. 6.10. continued

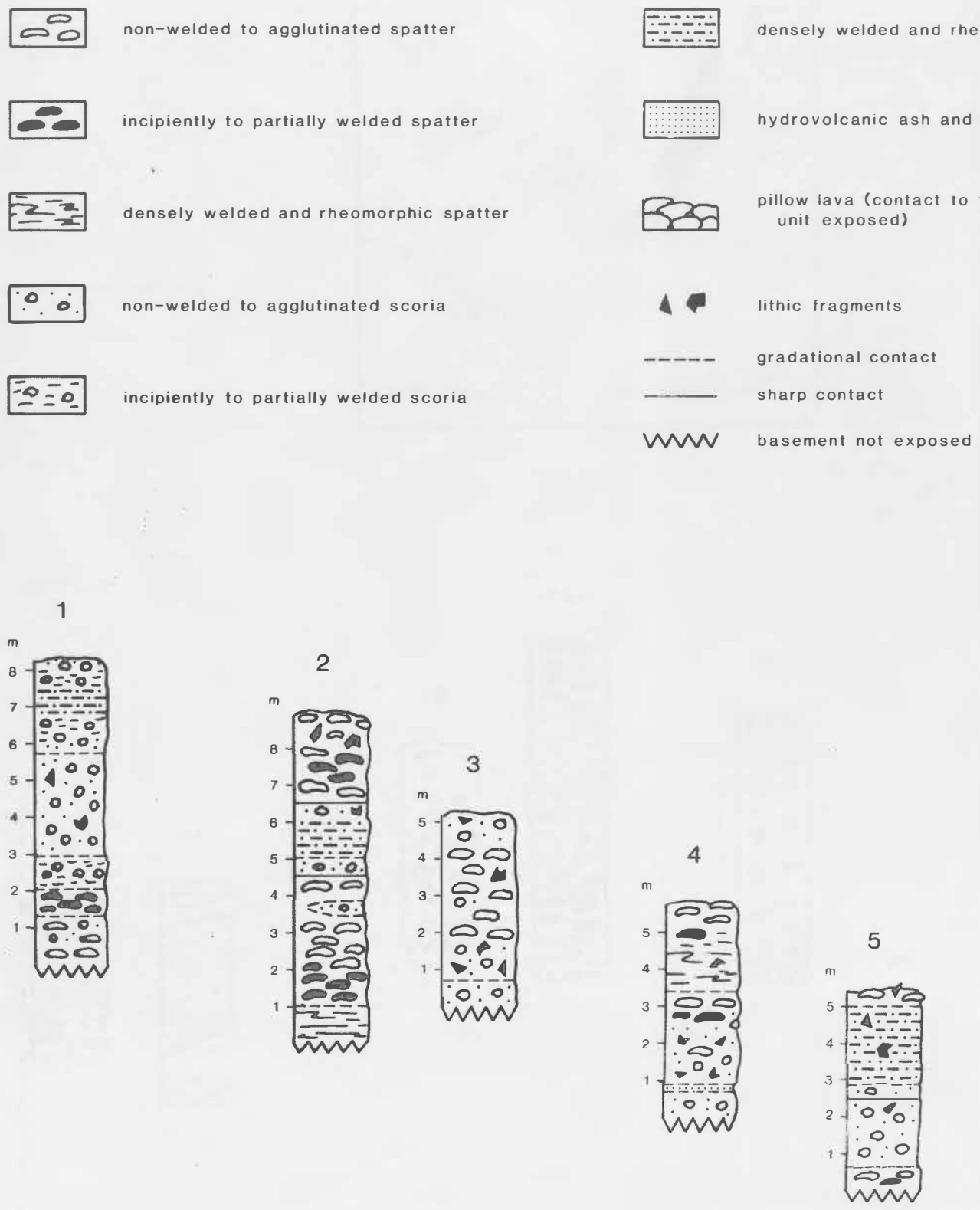

Fig. 6.11. Stratigraphy of the air-fall ejecta sho
sections parallel to the fissure. Sections 2, 5 and
based on the field notes by Th. Thordarson.

densely welded and rheomorphic scoria

hydrovolcanic ash and lapilli

pillow lava (contact to the overlying unit exposed)

lithic fragments

gradational contact

sharp contact

basement not exposed

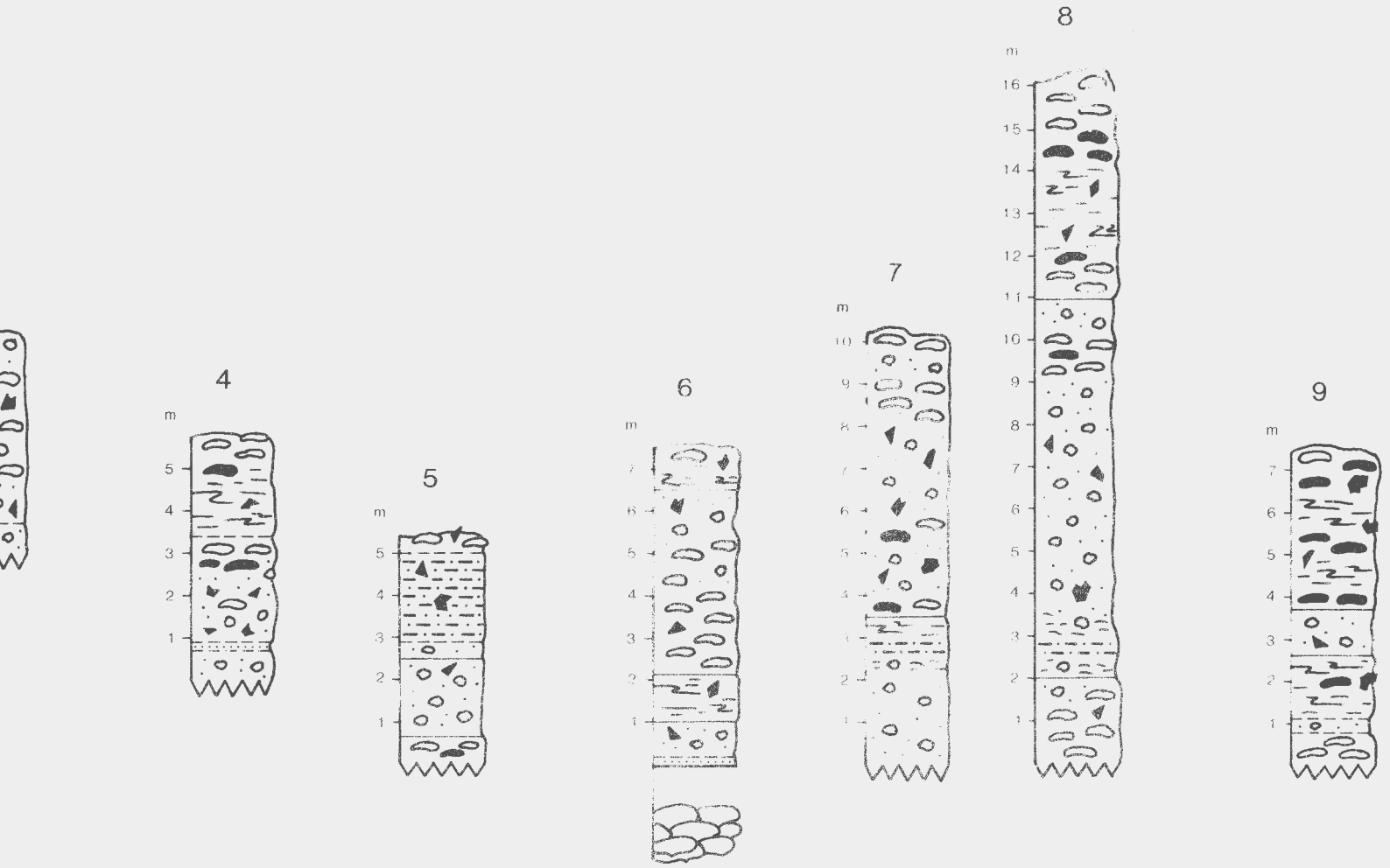

atigraphy of the air-fall ejecta shown in
llel to the fissure. Sections 2, 5 and 8 are
ield notes by Th. Thordarson.

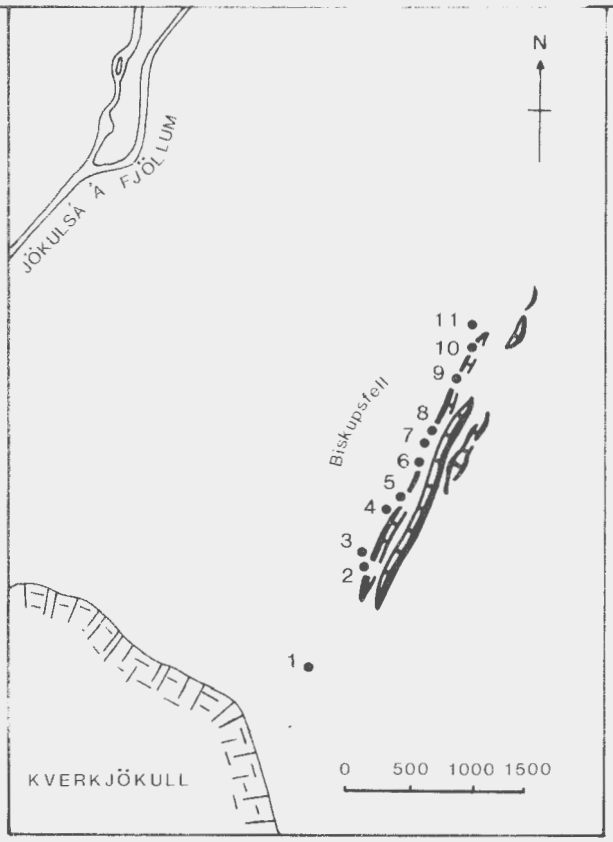
N
JÖKULSÁ Á FJÖLLUM
Biskupsfell
11
10
9
8
7
6
5
4
3
2
1
KVERKJÖKULL
0 500 1000 1500

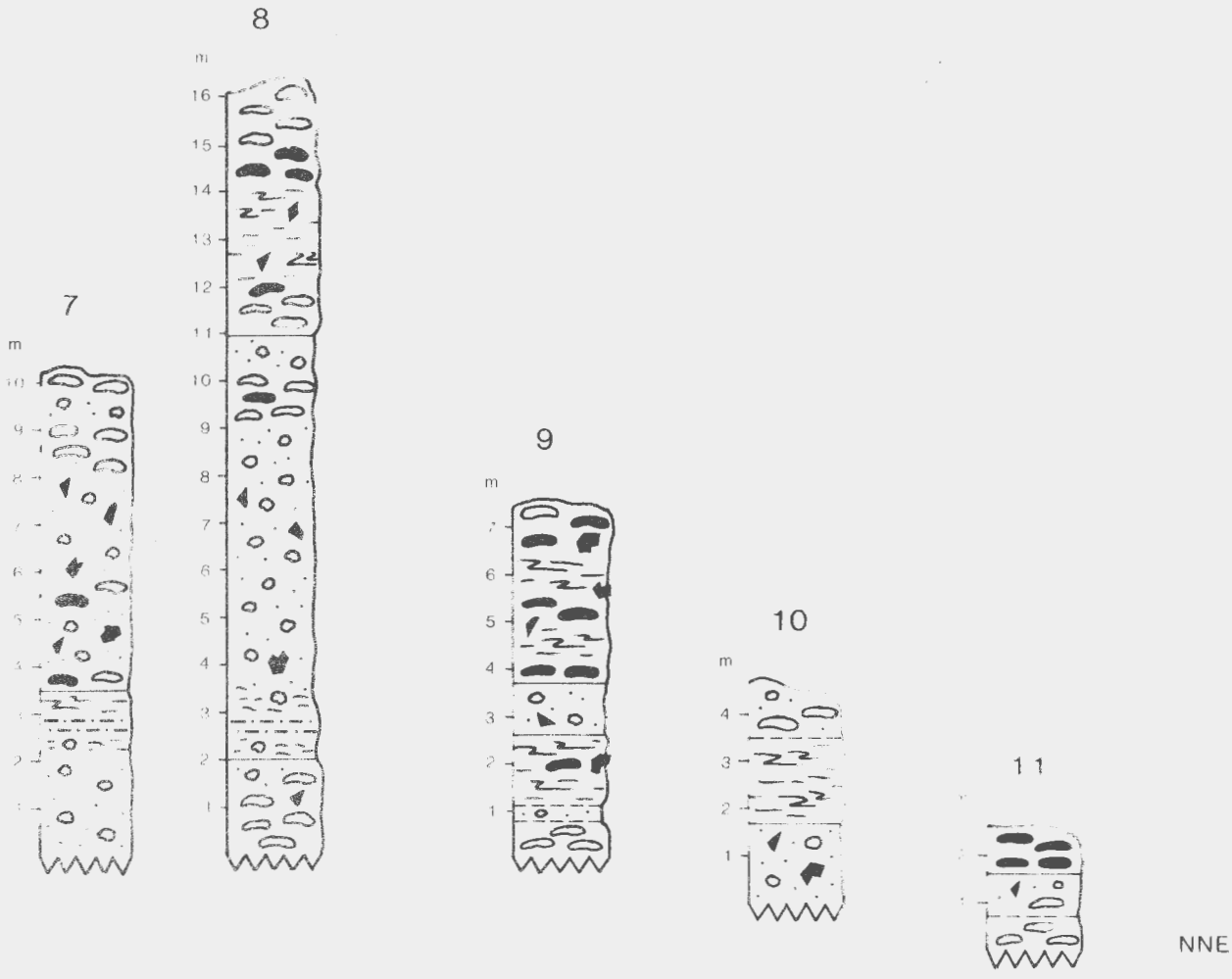
7
8
9
10
11
m
NNE

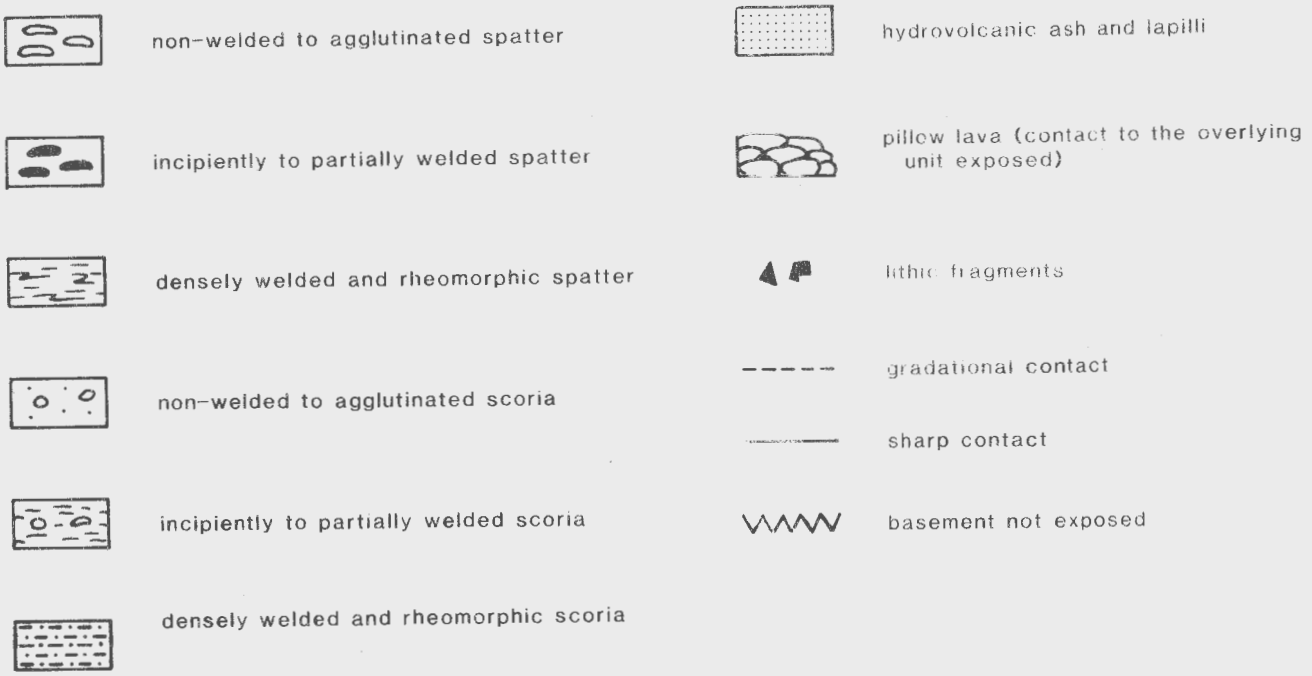

Fig. 6.12. Stratigraphy of the air-fall ejecta sections perpendicular to the fissure. Section 19 on the field notes by Th. Thordarson.

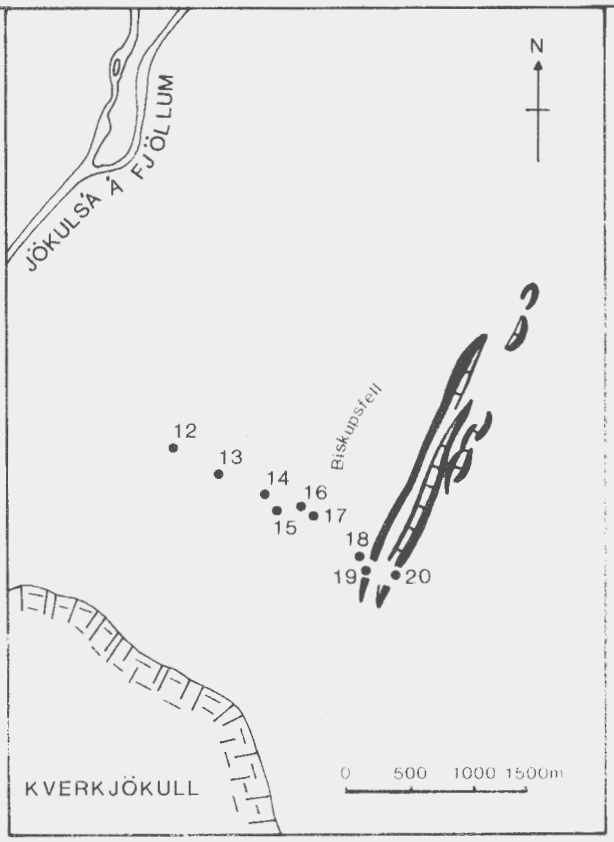

ydrovolcanic ash and lapilli

illow lava (contact to the overlying unit exposed)

ithic fragments

gradational contact

sharp contact

basement not exposed

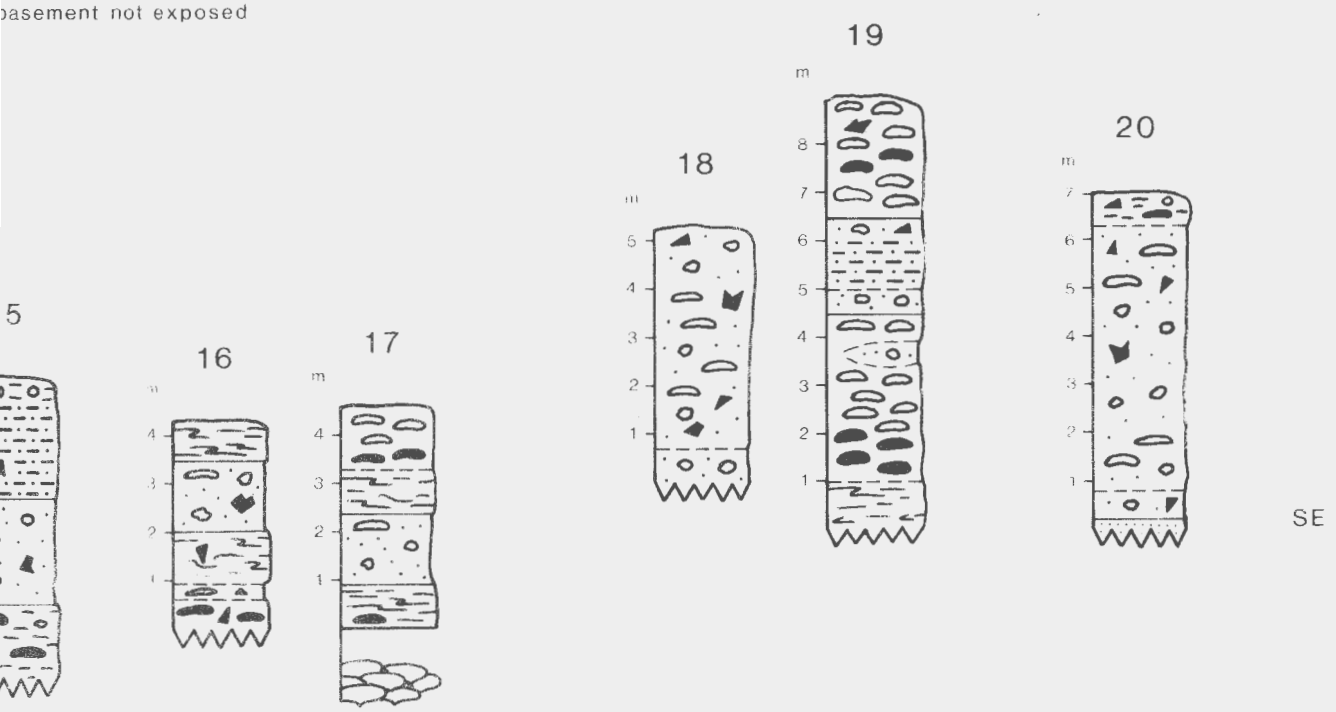

the air-fall ejecta shown in the fissure. Section 19 is based hordarson.

20m | vertical interval between the sections

were erupted; there is a sharp contact between those two deposits (Fig. 6.3., p. 28). The earlier mentioned pillow-like structures on the lava surface (Fig. 6.2., p. 28) also suggest a time interval long enough for some snow or ice to be formed before the last eruption phase took place.

In the southern end of the fissure a series of vent opened and thin lava flows were ejected through the earlier explosive craters. The distribution of the lava flows is shown in Fig. 6.7. (p. 39). The northern part of the fissure is marked by small spatter and scoria cone rows, also producing some thin and short lava flows. There is no direct contact between the ejected material from the southern part of the fissure and ejecta generated from the northern crater rows. Outpouring of ordinary lavas, however, marks the end phase of the eruption. The formation of the northern spatter and scoria cones with accompanying lava flows most likely dates in the last phase of the Biskupsfell eruption.

6.4. Estimate of the total erupted volume

An estimate of the total erupted volume during the Biskupsfell eruption has been made using the data in Figs. 6.7-6.10. The volumes erupted during the hydrovolcanic phase was calculated from data based on the field notes of Th. Thordarson. The volumes erupted during the main phase was calculated using the thickness isograds of each cycle. The areas covered by the rheomorphic and the ordinary lava flows were measured from the map shown in Fig. 6.7. (p. 39) and the volumes were estimated by multiplying the areas by

the average thicknesses of the respective flows. These estimates give the following values:

The hydrovolcanic ash		1.2 million cubic m
The Hawaiian-Strombolian deposits		30.5 million cubic m
I Hawaiian spatter	6	
Strombolian scoria	12.6	
II Hawaiian spatter	3.4	
Rheomorphic flows	8.5	
Ordinary lava flows		5.8 million cubic m
	total	37.5 million cubic m

The ejecta erupted during the Strombolian cycle consist mostly of unconsolidated, vesicular scoria as on the other hand the spatter deposits are more or less welded and give values which represent volumes of much denser material. The exposed rheomorphic flows for which the volume has been calculated are supposed to originate largely from the second Hawaiian fire fountain deposits. Stratigraphic sections show that the lower spatter deposits also include rheomorphic flows but their distribution and volume is unknown, indicating that the value of 6 million cubic m for the first Hawaiian spatter deposits is far too low. Of these estimates the value of 5.8 million cubic m of ordinary lava is the one probably nearest the true value representing the best exposed deposits. An addition of about one third to the calculated volume is suggested to give an estimate of the total erupted volume, giving a value about 50 million cubic m.

7. PETROLOGY AND MICROSCOPIC CHARACTERISTICS

7.1. Chemical composition of the glasses

The chemical composition of the glasses in the hydrovolcanic ash samples (except no. 3) is represented in Table 1. Sample locations are shown in Fig. 7.1. The analyses in Table 1 are of the glass phase only; the hydrovolcanically formed units consist mostly of glass shards and glassy, pumiceous lapilli. Pure glass is very rare in the other units. Small amounts of pure glass has been found in the topmost spatter unit (the second Hawaiian cycle), analysis no. 3 represents this glass phase.

TABLE 1

Chemical analyses of glasses from Biskupsfell

	SiO2	TiO2	Al2O3	FeOt	MnO	MgO	CaO	Na2O	K2O	P2O
1a	50.8	3.09	13.4	14.5	0.33	4.36	8.44	2.98	0.70	0.43
1b	51.0	3.02	13.5	14.2	0.36	4.26	8.35	3.00	0.71	0.43
1c	50.5	2.97	13.4	14.4	0.30	4.37	9.10	2.67	0.61	0.40
2a	49.3	2.92	13.4	14.6	0.25	4.86	9.29	2.16	0.61	0.36
2b	49.1	2.97	13.3	14.6	0.25	4.80	9.31	1.41	0.60	0.35
3	48.8	3.00	13.1	14.9	0.25	4.75	9.57	3.12	0.42	0.37

The analyses are of the natural glasses from the hydrovolcanic phase except no. 3, which is from a glassy top spatter erupted during the second Hawaiian fire fountaining cycle. Each analysis is an average of at least 10 spot analyses. Total Fe as FeOt.

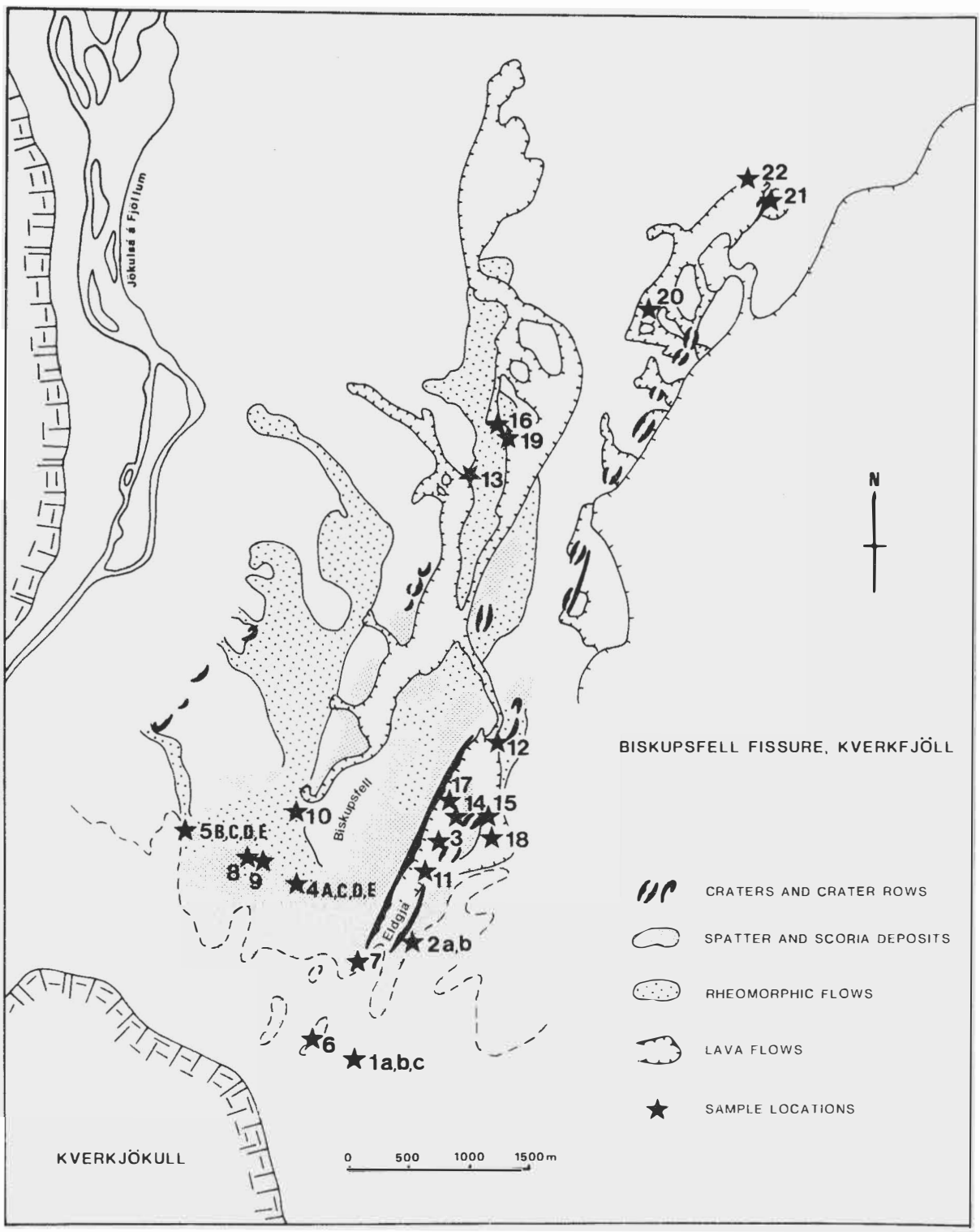

Fig. 7.1. Location map of the sample sites for the microprobe analyses.

To get whole rock analyses of the different air-fall units and of the lavas the samples were melted just above the liquidus, at 1200 C. These glasses were then analyzed on the microprobe. In Table 2 are listed the analyses of the air-fall ejecta erupted during the main eruption phase, the Hawaiian-Strombolian phase. Sample locations are shown in Fig. 7.1.

TABLE 2

Chemical analyses of fused glasses from Biskupsfell air-fall units

	SiO2	TiO2	Al2O3	FeOt	MnO	MgO	CaO	Na2O	K2O	P2O
4E	47.4	3.14	12.9	15.4	0.22	5.02	9.30	3.21	0.58	0.38
4D	47.8	3.01	12.9	15.7	0.23	4.89	9.27	3.17	0.60	0.41
4C	47.6	3.09	12.9	15.3	0.24	4.90	9.24	3.23	0.53	0.37
4A	49.5	2.96	13.1	15.3	0.24	4.99	9.47	3.14	0.59	0.39
5E	49.1	3.07	12.9	15.4	0.24	4.85	9.10	3.17	0.58	0.41
5D	48.8	3.11	12.4	15.3	0.26	4.96	9.34	2.98	0.61	0.40
5C	48.8	3.00	12.4	15.5	0.26	4.89	9.27	3.14	0.58	0.42
5B	48.5	3.13	13.1	15.3	0.22	5.01	9.36	3.07	0.57	0.38

The analyses are from the air-fall ejecta erupted during the Hawaiian-Strombolian phase. Each analysis is an average of at least 10 spot analyses. Total Fe as FeOt. The capital letters refer to a corresponding stratigraphical unit as follows:

E: the second Hawaiian cycle, spatter
D: the Strombolian cycle, scoria
C: the first Hawaiian cycle, the uppermost spatter
B: the first Hawaiian cycle, scoria lens
A: the first Hawaiian cycle, the lowermost spatter

Formation no. 4 is also represented in Appendix I corresponding to Section II.

In Table 3 is listed a group of occasional analyses representing only the topmost air-fall unit (spatter erupted during the second Hawaiian phase, corresponding the units E in Table 2) and the rheomorphic lavas, derived from the spatter formation concerned. Sample locations are shown in Fig. 7.1.

TABLE 3

Chemical analyses of fused glasses from Biskupsfell spatter units and rheomorphic flows

	SiO2	TiO2	Al2O3	FeOt	MnO	MgO	CaO	Na2O	K2O	P2O
6	49.1	3.17	13.1	14.5	0.26	4.21	8.44	3.29	0.69	0.48
7	50.1	2.93	13.3	14.4	0.25	4.94	9.31	2.91	0.59	0.39
8	51.7	2.69	12.4	13.6	0.26	4.89	9.17	2.53	0.62	0.45
9	50.1	2.86	13.2	14.5	0.24	4.84	9.26	2.96	0.59	0.42
10	49.7	2.99	13.0	14.5	0.24	4.83	9.23	2.97	0.54	0.39
11	48.7	2.85	13.3	14.5	0.23	4.91	9.30	3.14	0.55	0.39
12	48.3	3.00	13.4	14.8	0.24	4.95	9.45	3.10	0.54	0.40
13	50.1	3.07	13.2	15.3	0.23	5.04	9.42	3.01	0.54	0.38

Sample nos. 6-8 are analyses from the topmost air-fall ejecta erupted during the second Hawaiian cycle, and nos. 9-13 represent the rheomorphic lavas. Each analysis is an average of at least 10 spot analyses. Total Fe as FeOt.

In Table 4 is listed the composition of the ordinary lavas. During the last eruption phase Biskupsfell fissure produced two types of lavas. Small amounts of porphyritic lavas were first erupted in the southern part of the fissure. The latter lava flows are aphanitic. These lavas can be found both in the southern and northern part of the fissure. Sample locations are shown in Fig. 7.1.

TABLE 4

Chemical analyses of fused glasses from Biskupsfell lavas

	SiO2	TiO2	Al2O3	FeOt	MnO	MgO	CaO	Na2O	K2O	P2O
14	50.8	2.99	13.6	14.5	0.27	5.06	9.53	2.91	0.58	0.38
15	49.4	2.67	14.1	13.8	0.25	5.19	9.67	2.66	0.54	0.36
16	50.4	2.95	13.6	14.8	0.25	4.87	9.47	2.92	0.58	0.39
17	53.1	3.07	13.3	14.4	0.29	3.92	8.26	2.91	0.77	0.54
18	49.9	3.22	13.3	14.8	0.29	4.34	8.55	2.97	0.69	0.49
19	49.0	3.02	13.3	15.1	0.26	4.84	9.17	2.94	0.61	0.41
20	50.9	2.96	13.6	14.6	0.30	4.40	8.17	3.04	0.66	0.44
21	52.1	2.89	12.8	13.6	0.26	3.46	7.69	3.11	0.83	0.70
22	50.8	3.07	13.1	14.0	0.31	4.13	7.93	2.92	0.69	0.47

The first three analyses (nos. 14-16) are samples from the porphyritic lavas. The next three (nos. 17-19) represent the latter, aphyritic lavas erupted from the southern part of the fissure. The last three analyses (nos. 20-22) are lava samples representing the northern crater rows. Each analysis is an average of at least 10 spot analyses. Total Fe as FeOt.

7.2. Composition of the minerals

The minerals found in the Biskupsfell deposits are composed of microphenocrysts of plagioclase, olivine and minor augite. Some larger phenocrysts of plagioclase and olivine are present. The average composition of the minerals is given in Table 5. The individual analyses are listed in Appendix II. In many of the samples there is some variation in the plagioclase compositions; in these samples the different compositional populations are separated. Sample locations are shown in Fig. 7.1.

TABLE 5

The average composition of plagioclase.
Microphenocrysts.

	SiO2	Al2O3	FeOt	CaO	Na2O	K2O	An%
1b	52.5	30.3	1.45	13.4	4.20	0.14	65.2
1c(1)	54.3	28.9	1.19	12.0	4.71	0.16	59.7
(2)	51.7	31.5	0.77	14.2	3.58	0.09	69.2
3	49.2	28.3	1.31	11.3	4.09	0.16	62.0
4A(1)	56.2	25.8	1.01	9.34	6.42	0.45	45.5
(2)	53.0	25.5	1.10	11.4	5.36	0.24	55.0
(3)	50.8	28.7	0.89	13.4	4.09	0.13	65.1
(4)	49.5	28.7	0.79	14.4	3.52	0.13	69.6
4E(1)	57.8	22.2	1.22	7.38	6.36	0.96	59.6
(2)	53.9	27.6	1.17	11.4	5.18	0.26	56.0
(3)	51.9	26.6	1.10	13.9	3.48	0.18	69.4
5C(1)	51.4	30.2	0.83	13.1	3.80	0.09	66.3
(2)	50.3	30.5	0.68	14.2	3.30	0.10	70.7
8 (1)	56.5	25.3	1.78	8.95	5.66	0.31	49.4
(2)	55.0	28.5	1.32	11.2	4.69	0.24	58.1
9 (1)	54.5	28.3	1.25	11.2	4.75	0.20	58.0
(2)	51.8	30.3	0.81	13.3	3.57	0.09	67.9
14(1)	58.7	21.6	2.45	9.78	5.62	1.05	50.6
(2)	53.8	27.1	1.35	11.2	4.76	0.20	58.2
Phenocrysts.							
1b	47.5	34.4	0.63	17.7	1.89	0.11	83.6
1c	48.4	33.1	0.68	16.4	2.15	0.07	80.9
14	48.3	34.1	0.62	16.4	1.92	0.07	82.6

The average composition of olivine. Microphenocrysts.

	SiO2	FeOt	MgO	MnO	CaO	NiO	Fo%
1c	37.1	26.2	34.3	0.39	0.30	0.04	69.2
4A(a)	37.6	21.4	36.7	1.14	0.30	0.07	75.4
(b)	35.0	30.3	30.1	1.51	0.29	0.02	63.9
4E(a)	34.6	37.6	23.9	1.89	0.33	0.02	53.1
(b)	34.5	43.1	18.8	2.29	0.53	0.03	43.7
9	33.0	46.9	17.7	0.72	0.41	0.01	40.2
15	38.6	22.6	38.9	0.29	0.29	0.08	75.4
Phenocrysts.							
5C	37.4	26.2	35.4	0.41	0.25	0.01	70.6

The sample numbers refer to the corresponding glass analyses given in Tables 1-4. Total Fe as FeOt.

7.3. Temperature estimates

Different geothermometers have been used to estimate the approximate magma temperature on eruption assuming equilibrium crystallization. Olivine and plagioclase geothermometers have been examined, based on the compositions of olivine and liquid (glass) and of plagioclase and liquid (glass), respectively. The results are given in Table 6 (p. 59). The olivine phenocrysts in the samples are usually very small and their amount is low, which decreases the number of samples convenient for analyzing considerably. The plagioclase phenocrysts occur more uniformly and abundantly being more suitable for the microprobe analyses.

The distribution coefficient K_D between olivine and liquid was calculated to evaluate if the olivine crystals were in

equilibrium with the liquid. Since the glass analyses do not distinguish between Fe+3 and Fe+2 a value of Fe+3/Fe+2 ratio of 0.15 was assumed. The equation for calculating the distribution coefficient K_D is as follows (Roeder and Emslie 1970):

$$K_D = \frac{(X^{ol}_{FeO})\ (X^{liq}_{MgO})}{(X^{ol}_{MgO})\ (X^{liq}_{FeO})}$$

X = mole fraction

Previous studies indicate that equilibrium crystallization gives values close to 0.30 for olivine crystals and the liquid.

According to Roeder and Emslie (1970) the composition of olivine is dependent on the liquid composition only, as is the liquidus temperature. On this basis the equilibrium temperatures can be calculated using either the distribution of Mg or Fe between olivine and the liquid. Because only total Fe could be determined on the microprobe analyses only Mg distribution geothermometers have been used.

An olivine geothermometer by Roeder and Emslie (1970) gives the temperature of olivine equilibrium and is shown in Table 6, column 1. The experimental data used in developing this geothermometer is mainly based on Hawaiian basalts. A modification from Roeder and Emslie equation was made by Fisk et al. (1978), based on tholeiitic basalts from Reykjanes Ridge and Iceland. The results calculated using that modification are given in column 2, Table 6.

TABLE 6

Temperature calculations using microphenocryst and glass composition

	1	2	3	4		K_D
1b				1155	C	
1c	1121	1075	1082		C	0.28
(1)				1116	C	
(2)				1132	C	
3				1145	C	
4A(a)	1132	1087	1094		C	0.22
(b)	1169	1128	1139		C	0.37
(1)				1066	C	
(2)				1110	C	
(3)				1159	C	
(4)				1184	C	
4E(a)	1226	1195	1210		C	0.58
(b)	1285	1263	1285		C	0.86
(1)				1051	C	
(2)				1122	C	
(3)				1190	C	
5C(1)				1163	C	
(2)				1188	C	
8 (1)				1053	C	
(2)				1096	C	
9	1283	1261	1283		C	1.04
(1)				1118	C	
(2)				1167	C	
14(1)				1091	C	
(2)				1117	C	
15	1140	1096	1104		C	0.25

Temperature calculations using phenocryst and glass composition

1b				1274	C	
1c				1240	C	
5C	1141	1097	1106		C	0.26
14				1259	C	

A comparison of calculated temperatures using the following methods:

1) Olivine temperature using equation from Roeder and Emslie (1970).
2) Olivine temperature using equation from Fisk et al. (1978).
3) Olivine temperature using equation from Grönvold (1984), see text.
4) Plagioclase temperature using equation from Grönvold (1984), see text.

The sample numbers refer to the corresponding glass and mineral analyses.

A third equation for the Mg distribution between olivine and basaltic liquid is based on some experimental results from Krafla lavas, north Iceland (Grönvold 1984). The geothermometer is as follows:

$$\log \frac{X^{ol}_{MgO}}{X^{liq}_{MgO}} = \frac{2927}{T^{\circ}} - 1.349$$

X^{ol}_{MgO} mole fraction MgO in olivine

X^{liq}_{MgO} = mole fraction MgO in glass

The calculated olivine temperatures using this equation are shown in column 3, Table 6.

The K_D values of the olivine geothermometers vary drastically as shown in Table 6. This indicates that most of the olivine crystals were not in equilibrium with the liquid by the time of crystallization and this limits the use of these olivine geothermometers. Especially the high temperatures, over 1280 C with the corresponding high K_D values, look like due to xenocrysts. The samples 1c, 5C and 15 with the K_D values 0.25 to 0.28, are in relatively good agreement with the results of Roeder and Emslie (1970) and could be considered to give values close to the equilibrium temperatures, 1082-1106 C, for the corresponding olivines.

Kudo and Weill (1970) formulated a geothermometer based on plagioclase - liquid equilibrium. The same experiments from Krafla lavas that were used for the olivine geothermometer (above) produced a plagioclase geothermometer modified after Kudo and Weill (Mäkipaa, in Grönvold 1984). The equation is as follows:

$$\ln \lambda/\delta + 8.06\times10^{3}\ \Phi'/T = 9.95\times10^{-3}\ T - 15.03$$

$$\lambda = x_{Na}x_{Si}/x_{Ca}x_{Al};\quad \delta = X_{Ab}/X_{An};\quad \Phi' = x_{Ca} + x_{Al} - x_{Na} - x_{Si}$$

x = atomic fraction in the liquid

X = mole fraction in plagioclase

T - 273.15 = T in °C

The plagioclase crystallization temperatures using this equation are shown in column 4, Table 6. Appendix II gives the individual analyses of plagioclases and olivines and their corresponding crystallization temperatures calculated by means of the two equations given above. As shown in the glass analyses (Tables 1-4) there is no significant chemical variation between the whole rock samples (fused glass) and the natural glass samples. This indicates that the composition of the liquid was not affected by the amount of microphenocrysts. Accordingly, the crystallization temperatures calculated by means of fused glass (samples 4A, 4E, 5C, 8, 9, 14, 15) instead of natural glass (samples 1b, 1c) can be considered to give a temperature value of about the same accuracy as the natural glasses gives.

The plagioclase geothermometer is though considered to be less accurate than the olivine geothermometer. The great scatter of the calculated plagioclase temperatures indicates that all the plagioclases were not in equilibrium with the liquid. An average of the plagioclase temperatures, 1127 C, falls, however, very near the calculated temperatures for Myvatn lavas 1724-1729, north Iceland, and are somewhat lower than the temperature estimates for some Krafla lavas

from north Iceland, erupted 1975 and 1977 (Grönvold 1984; Grönvold & Mäkipaa 1978, resp.).

Most of the samples are very fine-grained and show evidence of rapid cooling and quenching. The low crystallinity indicates that the magma temperature on eruption was close to the liquidus temperature. The average olivine temperature is estimated as about 1100 C and the average plagioclase temperature as about 1130 C. The temperature estimates, about 1260 C, from the phenocrysts in sample no. 14 (the porhyritic lava erupted during the last phase) obviously give the temperature at the magma reservoir.

7.4. Microscopic characteristics

The mineralogy of the Biskupsfell deposits is relatively simple. The studied samples are mostly composed of microphenocrysts of plagioclase, olivine and augite in a very fine-grained matrix of plagioclase and opaque glass. Plagioclase phenocrysts are relatively rare in the non-welded and agglutinated units, in the densely welded zones the phenocrysts appear slightly more abundant due to compaction and flattening resulting a higher concentration of phenocrysts per unit volume in the welded layers.

Lithic fragments can be distinguished from the essential material in thin sections. There is usually a thin (0.5 - 1 mm), dark, chilled margin around the lithic fragments and the mineral composition is usually different from the essential material.

7.4.1. Non-welded and incipiently welded units

The non-welded and slightly welded units are usually highly vesicular with spherical or ellipsoidal vesicles. The texture varies between sub-ophitic and intergranular with skeletal plagioclase needles and laths in a matrix of predominantly opaque glass and very fine-grained plagioclase, olivine and clinopyroxene crystals. Some glomeroporphyritic aggregates with intergrowth of plagioclase, olivine and augite appear here and there in the fine-grained matrix. The olivine microphenocrysts have usually a skeletal crystal texture.

7.4.2. Welded units

The welded units are usually composed of very fine-grained material. The matrix contains mostly of a mass of opaque, black glass, microphenocrysts of plagioclase, and some just recognizable olivine and augite crystals. The plagioclase microphenocrysts have often a skeletal crystal texture. In some places a few plagioclase grains form glomeroporphyritic aggregates with smaller olivine and augite grains. A beginning of spherulitic texture is visible in a few samples. The plagioclase needles tend to be placed along the foliation plane of the unit. Larger euhedral plagioclase phenocrysts are rare.

The rheomorphic units have a very similar microtexture as the welded units except for a marked flow texture. The matrix is often hyalopilitic composed predominantly of

opaque glass. Larger plagioclase phenocrysts are rare, but microphenocryst of plagioclase, olivine and augite are present. The needle-shaped plagioclase crystals are usually aligned in the flow direction indicating that they were formed just before or at the same time with the deposition of the rheomorphic flows.

7.4.3 Lava flows

The Biskupsfell lavas erupted during the last eruption phase are of two types. The earlier lava is characterized by plagioclase phenocrysts, while the latter one is aphyritic. Both lavas are highly vesicular with rounded vesicles, often elongated in the flow direction. The matrix is also very similar in both lavas. They have an intergranular to sub-ophitic texture consisting of small olivine crystals and grains of opaque glass intergrown with lath-like or needle-shaped plagioclase crystals. Both the plagioclase and olivine crystals usually have a skeletal texture with a central cavity. A pronounced flow texture in both lavas appears by the plagioclase needles aligned parallel to the flow direction. Phenocrysts in the earlier erupted lava consist mostly of euhedral plagioclase grains, some of them have been broken. A few olivine phenocrysts are also present.

7.5. Quench crystallization and supercooling

There is a marked correlation between the cooling rate and the crystal morphology. The small grain size ranging downwards to partly glassy material in the deposited units ows its origin to a rapid supercooling. At significant degrees of supercooling, plagioclase has relatively higher nucleation rate but slower growth rate compared to augite (Hughes 1982). This results a sub-ophitic or ophitic texture with plagioclase microlites partially or wholly enclosed by augite. Under higher degrees of supercooling the extrusive material can have readily nucleated pyroxene in addition to plagioclase, resulting an intergranular texture with pyroxene prisms and grains of opaque minerals between tabular microlites of plagioclase (Hughes 1982). The matrix textures through the Biskupsfell spatter and scoria units varies mainly from intergranular and hyalopilitic to sub-ophitic with skeletal plagioclase needles and/or laths in a matrix of opaque glass and very fine-grained crystal mass of plagioclase, olivine and augite.

Most of the plagioclase microphenocrysts throughout the units have skeletal or quench crystal textures. The few olivine and augite grains are also often skeletal. The skeletal crystal texture can be used as an indication of the degree of cooling of the magma during the eruption. Lofgren (1974) has done a thorough experimental study of the systematic variation of plagioclase morphology related to the degree of cooling. Other work on crystal morphology of plagioclase and olivine agrees with Lofgrens experimental

results and interpretation (Kirkpatrick 1975; Donaldson 1976; Gutmann 1977; Hughes 1982). In Lofgrens experiments the samples were first melted, and then the temperature was rapidly dropped to some predetermined value below the liquidus. The difference between the liquidus temperature Tr and the crystallization temperature Tg gives Δ T, the degree of supercooling. The plagioclase morphology is markedly dependent on the degree of supercooling, Δ T, changing from tabular crystals at small Δ T values to skeletal crystals, dendrites, and spherulites with progressively increasing Δ T values.

In Lofgrens (1974) experiments acicular or skeletal plagioclase crystals were found at Δ T values between 100 and 200 C, depending on composition. Tabular crystals up to 2 mm were found at Δ T values of less than 100 to 150 C. Those crystals were homogeneous and generally equant. The Δ T values associated with the crystal morphologies were done with compositions of An60 or less. The plagioclase microphenocrysts analyzed from the Biskupsfell air-fall deposits have an average composition of about An60. In some of the spatter units microphenocryst populations with higher Ab-content were found. The composition of the plagioclase in those units is andesitic with An45-56. Prominently the plagioclase microphenocrysts resemble Lofgrens experiments acicular, skeletal types. This would then indicate a drop of temperature of about 100 up to 200 C during the accumulation of the ejecta. Assuming the initial eruption temperature as about 1100-1130 C (p. 62) a temperature drop of 100 to 200 C would then give the temperature after the accumulation as

1000-1030 to 900-930 C, respectively. Experiments on rhyolitic tuffs indicate that welding can take place in relatively low temperatures, between about 600 and 750 C (Ross & Smith 1961; Friedman et al. 1963). The temperature drop from about 1100 C to as low as 900 C during the accumulation would not yet be large enough to inhibit welding of the deposited ejecta.

Large phenocrysts are rare in the spatter and scoria deposits and in the rheomorphic flows derived from them. The plagioclase crystals present are usually zoned at their margins and some of them show marginal resorption. Through all the units, from non-welded to densely welded and rheomorphic spatter, the plagioclase microphenocrysts appear as acicular, skeletal needles and/or laths often with corroded crystal boundaries. The corroded crystal boundaries indicate a disequilibrium between the crystals and the melt. The disequilibrium between some of the plagioclase crystals and the liquid was stated earlier in the connection with the calculated plagioclase temperatures (p. 59, 61).

8. ERUPTION MECHANISM AND RHEOMORPHISM

The three distinctive eruption phases in Biskupsfell, the hydrovolcanic, the Hawaiian-Strombolian and the lava flow phase are all different concerning the nature of ejecta and the amount of erupted material. The Hawaiian-Strombolian phase clearly forms the main phase of the whole eruption. It is also the most variable and complicated regarding both the

eruption mechanism and the resulting ejecta. The deposits formed during the Hawaiian-Strombolian phase are products of very powerful lava fountaining and of more explosive activity. The whole 3 km long southern end of the fissure probably acted as an initial eruptive vent. However, the locations of the air-fall deposits and their relation to each other suggest that the activity along the fissure was from time to time localised to a number of separate vents.

The eruption products ejected during the main eruption phase clearly show a cyclic variation as the eruption proceeded. All the events were more or less explosive, producing air-fall material. The eruptive episodes can roughly be divided into more explosive Strombolian and less explosive Hawaiian cycles. Three relatively distinct, powerful eruptive cycles can be traced through the depositional sequences, from below upwards: a Hawaiian cycle, a Strombolian cycle and a second Hawaiian cycle. The deposits originating from these eruptive cycles can be found in a number of sections in the western Biskupsfell area. The accumulated ejecta around some of the smaller vents does not show this threefold division; these vents probably acted as short-lived Strombolian explosive centers producing very localised scoria deposits. The eruptive cycles have been partly transitional in style, with both the Strombolian and the Hawaiian mechanism operating in rapid succession or simultaneously in separate vents.

During the less explosive, Hawaiian eruptions, the eruption column forms a lava fire fountain or 'curtains of fire' when the eruption occurs along a linear fissure. During the fire fountaining a high proportion of lava spatter is ejected

through the vent. A considerable part of the lava spatter usually falls back to the vent or around the vent area, forming local spatter cones and spatter ramparts. According to Macdonald (1972) the Hawaiian lava fountain heights are generally less than about 200 meters, and in such cases magma would be ejected at velocities of a few tens of meters/s (Wilson & Head 1981). Two recorded examples of Icelandic basaltic activity give fire fountain heights of 50 to 100 m for the 1973 Heimaey eruption (Thorarinsson et al. 1973) and 300 to 500 m for the 1961 Askja eruption (Thorarinsson & Sigvaldason 1962) and are considered to be typical for Icelandic basaltic activity.

In the Biskupsfell area large spatter bombs exceeding 0.5 meter in diameter can be found at a distance over 1 km W from the fissure, and meter-sized spatter bombs are situated in locations over half a kilometer from the vents. These bombs are situated where originally deposited, on hill tops, so their present location cannot be due to rheomorphic flow. The surrounding hills where these lava spatter can be found, are situated at elevations about 50 to 100 m above the present Eldgjá valley bottom. The mountain Biskupsfell, situated on the western side of the main fissure, rises about 120 to 140 m above the subjacent Eldgjá valley. Air-fall spatter deposits can be found on the top of the mountain and also on locations behind Biskupsfell. However, there the thicknesses of the spatter units, except for rheomorphic flows, are less than on corresponding areas farther south. Probably the mountain Biskupsfell acted as a barrier for some of the less powerful fire fountain

episodes. Fire fountaining at Eldgjá is supposed to have reach heights of about 150 to 250 meters.

During the lava fountain stages the magma discharge rate must have been very high to explain the development of the high amount of welded deposits. During some fire fountain stages at Kilauea 1983-1988 activity lava discharge rate was 100 to 500 cubic m/s and the fire fountain height was 500 m (G. P. L. Walker, pers.comm.). According to Walker welded tuffs developed then only within about 0.5 km from the vent. Air-fall spatter erupted from the Biskupsfell fissure have developed intensive welding at distances about 1 km from the vent. All this indicates that the fire fountaining, although relatively low, have been very powerful with an extremely high discharge rate, perhaps from 5000 to as high as 10000 cubic m/s. Strong easterly and northeasterly winds accompanied the lava fountaining distributing a good deal of the ejecta to west and southwest.

The more explosive, Strombolian eruption cycles are driven by the explosive release of magmatic gas. Some of the explosive bursts were very likely caused by the interaction of magma and surface water, in this case by the melt water from the glacier or from some isolated snow patches along the fissure. Thin, highly vesiculated, fine-grained lapilli layers between the ordinary scoria and spatter deposits indicate this origin. Small amounts of surface water could have been accessible during most of the Hawaiian-Strombolian phase thus contributing the explosive strength of the eruption.

Strombolian explosions are thought to have generated when large gas bubbles (<1 to >10 m in diameter) burst at the surface of magma (Blackburn et al. 1976). The rate at which magma rises to the surface is of importance because it has also a great effect on the bubble formation and bubble rise. As an erupting magma approaches the surface the pressure in the magma decreases and volatiles begin to nucleate to form bubbles (Fisher & Schmincke 1984). The bubbles grow either until they are inhibited by neighboring bubbles or until they reach the level of magma disruption. The dynamics of bubble growth depends largely on the following factors bubbles grow fastest for

1) low rates of magma ascent,
2) high diffusion coefficients,
3) high volatile content,
4) low values of the solubility constant, i.e. the quantity of volatiles that can be dissolved in the magma (Sparks 1978).

The bubble growth increases the efficiency of vesiculation and magma disruption and thus decreases the mean gas pressure during the magma ascent. The pressure drop decreases the magma rise rate and the nucleated gas bubbles have time to coalesce with smaller bubbles. The resulting increase in bubble volume will lead to an increase in rise speed of the bubbles (Wilson & Head 1981). The growth of gas bubbles leading to increased bubble-rise velocity clearly develops a runaway situation where very large bubbles arrive intermittently at the magma surface. When the bubbles can move through the magma at a rate greater than the magma

ascent discrete explosions typical of Strombolian type of eruptions commonly take place (Wilson & Head 1981). This happens when the rise velocity of the ascending magma is less than 0.5 m/s.

During the explosions the erupting magma is probably in variable stages of degassing. This factor explains the variety of the explosive material, ranging from highly vesicular scoria to dense, poorly vesiculated bombs. Some pauses in activity were likely to occur, and at least a short pause seemed to have occurred between the first Hawaiian lava fountaining and the following Strombolian explosive episodes. During such pauses in activity a crust has time to form on the magma surface (Wilson 1980a). During the next explosive episodes this partly consolidated crust will be ejected together with the fragmented lava clasts. This mechanism explains the occurrence of the large, dense lava blocks found in some of the Strombolian scoria units. In many of the Strombolian scoria units high concentrations of lithics, derived mostly from the local moraine cover, are present. As indicated earlier the high lithic content at least partly could have inhibited the development of intensive welding in some of the scoria units.

Hawaiian type eruptions are supposed to occur if the magma rise velocity at depth is greater than 1 m/s (Fisher & Schmincke 1984). Under these circumstances the gas bubbles are small and a steady fire fountain will be formed. If the magma outflow rate is large and the grain size of the magma clots is sufficiently small, the fire fountain is optically thick and cooling rate very slight. On landing the magma

clots will usually coalesce to form a lava flow (Head & Wilson 1986). In optically thin fire fountaining some cooling of all clots will occur. The amount of cooling depends on the initial temperature of the magma, on the grain size of the clots and on flight time. The result will be a non-welded air-fall scoria deposit, a slightly to densely welded spatter deposit or a formation of a lava flow caused by the coalescing of the air-fallen magma clots, a rheomorphic lava flow.

Most of the spatter deposits of Biskupsfell show a pronounced degree of welding and features indicating rheomorphism. Many of the layers are welded even in places where they are not more than 1 meter thick, situated on the very top of the formation. Therefore, lithostatic loading was relatively unimportant in controlling the welding. High initial eruption temperature, about 1100 to 1130 C, and, in particular, the absence or insignificance of any cooling of the spatter fire fountains during the Hawaiian eruption cycles were clearly more important. The fire fountain columns were probably dense enough to allow sufficient heat to be retained in the accumulated deposits to produce the observed degree of welding. Crystal morphologies suggest a drop of temperature of about 100 to 200 C during the deposition of the spatter and scoria units. Experimental studies indicate that welding can take place in rhyolitic tuffs at temperatures as low as about 580 C, and many rhyolitic pumices have been found to weld at temperatures between about 600 to 750 C (Ross & Smith 1961; Friedman et al. 1963). Corresponding experiments on basaltic tuffs are

not available. However, a temperature drop of 100 to as much as 200 C from the original 1100-1130 C during the deposition of the Eldgjá deposits would still be insufficient to inhibit the welding.

9. SUMMARY

Welded tuffs and ignimbrites of acid and peralkaline composition have been well described in literature from many parts of the world. Biskupsfell formation is one of the few studied and described basaltic air-fall deposits which shows both intense welding and rheomorphic flowing of the welded units.

The eruption of Biskupsfell shows a marked cyclicity in the type of ejecta, and this can be followed through the depositional sequences. The initial stage of the eruption was an explosive interaction between surface water and magma and highly fragmented tephra deposits were formed. After the glacial melt water supply was depleted there was a marked change in the eruption style. In the beginning of the main eruption phase small amounts gas-rich magma was ejected forming thinner scoria beds now underlying the main Hawaiian-Strombolian formation. Then the magma ascent velocity probably increased considerably and gas-poor magma was ejected with a very high discharge rate. During the magma ascent the mean gas pressure decreases in the magma chamber. Magma rise velocity decreases and probably the whole eruption stopped for a short while. Gas bubbles have now time to coalesce and grow resulting an increasing rise

speed of the bubbles. Strombolian explosive episodes are ready to occur.

After some time the magma rise velocity for some reason increased again considerably. Probably the gas-rich magma was depleted on the top of the magma chamber and the mean pressure in the chamber started to increase. The second Hawaiian fire fountaining with a high discharge rate characterizes the last episodes of the main eruption phase. The third eruption phase was marked by simply upwelling of fluid basaltic lavas through the previous explosive vents.

During the main eruption phase the discharge rate probably fluctuated in separate vents, the longest and the most powerful episodes being responsible for the three pronounced eruption cycles with their characteristic ejecta. During shorter change-overs in the eruption style thinner bed and lenses with different morphological clast characteristics were deposited. The total thickness of all air-fall ejecta amounts to over 16 m along the Eldgjá valley and to over 6 m on locations about 1 km WSW from the fissure. A great amount of the ejecta was blown west and southwest by strong easterly and northeasterly winds.

The basic controls of welding seem to have been high discharge and high accumulation rates of the pyroclasts during the Hawaiian lava fountain phases. A dense fire fountain cloud loses very little of its heat because the heat radiated from each particle is absorbed by its neighbours. Rapid accumulation also prevents cooling in the deposited fragments which quickly become insulated by the

following hot pyroclasts. Accordingly, during the Biskupsfell fires a relatively low, about 150 to 250 m heigh, but very dense fire fountaining with exceptionally high discharge rates, probably from 5000 to as high as 10000 cubic m/s, seemed to have been the case. This mechanism is ideal for retaining high temperature in the ejected pyroclasts which then during accumulation are capable to produce an intense welding. Accumulated on mountain slopes the welded units became unstable and flowed down as rheomorphic flows following the topographic lows.

Acknowledgements

This project was suggested to me by Dr. Karl Grönvold for my two and a half years fellowship at the Nordic Volcanological Institute in Reykjavik, Iceland, supported by the Nordic Council. Dr. Karl Grönvold is acknowledged for introducing me to the field, supervising the study and critically reading several versions of the manuscript, and for suggested improvements. Mr. Thorvaldur Thordarson is acknowledged for many helpful advice and ideas during the field work. Professor Carl Ehlers from Åbo Akademi is acknowledged for critically reading the manuscript. The staff at the Nordic Volcanological Institute is thanked for all their help during my stay in Iceland.

REFERENCES

Björnsson, S. and Einarsson, P., 1974. Seismicity of Iceland. In Kristjansson, L. (ed.). Geodynamics of Iceland and the North Atlantic Area. D. Reidel Publishing Company, Dordrecht, Holland. 225-239.

Blackburn, E.A., Wilson, L. and Sparks, R.S.J., 1976. Mechanisms and dynamics of Strombolian activity. J. Geol. Soc. London, 132, 429-440.

Cas, R.A.F. and Wright, J.V., 1987. Volcanic Successions. Modern and ancient. Allen & Unwin Ltd., London. 528 pp.

Chapin, C.E. and Lowell, G.R., 1979. Primary and secondary flow structures in ash-flow tuffs on the Gribbles Run paleovalley, central Colorado. In Chapin, C.E. and Elston, W.E. (eds.). Ash-Flow Tuffs. Geol. Soc. Am. Spec. Paper, 180, 137-154.

Donaldson, C.H., 1976. An Experimental Investigation of Olivine Morphology. Contrib. Mineral. Petrol., 57, 187-213.

Eichelberger, J.C. and Koch, F.G., 1979. Lithic fragments in the Bandelier Tuff, Jemez Mountains, New Mexico. J. Volcanol. Geotherm. Res., 5, 115-134.

Fisher, R.V., 1961a. Proposed classification of volcaniclastic sediments and rocks. Geol. Soc. Am. Bull., 72, 1409-1414.

Fisher, R.V. and Schmincke, H.-U., 1984. Pyroclastic Rocks. Springer-Verlag, Berlin. 472 pp.

Fisk, M. R., Schilling, J.-G. and Sigurdsson, H., 1978. Olivine geothermometry of Reykjanes Ridge and Iceland Tholeiites. EOS (abstract), 59, 410.

Friedman, I., Long, W. and Smith, R. L., 1963. Viscosity and water contents of rhyolite glass. J. Geophys. Res., 68, 6523-6535.

Grönvold, K., 1984. Myvatn fires 1724-1729. Chemical composition of the lava. Nordic Volcanological Institute, 8401. 24 pp.

Grönvold, K. and Mäkipaa, H., 1978. Chemical composition of Krafla lavas 1975-1977. Nordic Volcanological Institute, 7816. 49 pp.

Gutmann, J.T., 1977. Textures and genesis of phenocrysts and megacrysts in basaltic lavas from the Pinacate volcanic field. Am. J. Sci., 277, 833-861.

Head, J. W. and Wilson, L., 1986. Volcanic processes and landforms on Venus: theory, predictions, and observations. J. Geophys. Res., 91, 9407-9446.

Hughes, C.J., 1982. Igneous Petrology. Elsevier Scientific Publishing Company, Amsterdam. 551 pp.

Kirkpatrick, R.J., 1975. Crystal Growth from the Melt: A Review. Am. Mineral., 60, 798-814.

Kudo, A. M. and Weill, D. F., 1970. An igneous plagioclase thermometer. Contrib. Mineral. Petrol., 25, 52-65.

Lofgren, G., 1974. An experimental study of plagioclase crystal morphology: isothermal crystallization. Am. J. Sci., 274, 243-273.

Macdonald, G. A., 1972. Volcanoes. Prentice-Hall, Inc., Englewood Cliffs, New Jersey. 510 pp.

Peterson, D.W., 1979. Significance of the flattening of pumice fragments in ash-flow tuffs. In Chapin, C.E. and Elston, W.E. (eds.). Ash-Flow Tuffs. Geol. Soc. Am. Spec. Paper, 180, 195-204.

Ragan, D.M. and Sheridan, M.F., 1972. Compaction of the Bishop Tuff, California. Geol. Soc. Am. Bull., 83, 9-106.

Roeder, P. L. and Emslie, R.F., 1970. Olivine liquid equilibrium. Contrib. Mineral. Petrol., 29, 275-289.

Ross, C.S. and Smith, R.L., 1961. Ash-Flow Tuffs: their origin, geologic relations and identification. U.S. Geol. Surv. Prof. Paper, 366. 81 pp.

Schmincke, H.-U. and Swanson, D.A., 1967. Laminar viscous flowage structures in ash-flow tuffs from Gran Canaria, Canary Islands. J. Geol., 75, 641-664.

Sigvaldason, G. and Steinthorsson, S., 1974. Chemistry of tholeiitic basalts from Iceland, and their relation to the Kverkfjoll hot spot. In Kristjansson, L. (ed.). Geodynamics of Iceland and the North Atlantic Area. D. Reidel Publishing Company, Dordrecht, Holland. 155-164.

Smith, R.L., 1960a. Ash Flows. Geol. Soc. Am. Bull., 71, 795-842.

Sparks, R.S.J., 1978. The dynamics of bubble formation and growth in magmas: a review and analysis. J. Volcanol. Geotherm. Res., 3, 1-37.

Sparks, R.S.J. and Wright, J.V., 1979. Welded air-fall tuffs. In Chapin, C.E. and Elston, W.E. (eds.). Ash-Flow Tuffs. Geol. Soc. Am. Spec. Paper, 180, 155-166.

Thorarinsson, S. and Sigvaldason, G., 1962. The eruption in Askja, 1961. A preliminary report. Am. J. Sci., 260, 641-651.

Thorarinsson, S., Steinthorsson, S., Einarsson, T., Kristmannsdottir, H. and Oskarsson, N., 1973. The eruption of Heimaey, Iceland. Nature, 241, 372-375.

Walker, G.P.L., Self, S. and Wilson, L., 1984. Tarawera 1886, New Zealand - a basaltic plinian fissure eruption. J. Volcanol. Geotherm. Res., 21, 61-78.

Wilson, L., 1980a. Relationships between pressure, volatile content and ejecta velocity in three types of volcanic explosion. J. Volcanol. Geotherm. Res., 8, 297-313.

Wilson, L. and Head, J. W., 1981. Ascent and eruption of basaltic magma on the Earth and Moon. J. Geophys. Res., 86, 2971-3001.

Wolff, J.A. and Wright, J.V., 1981a. Rheomorphism of welded tuffs. J. Volcanol. Geotherm. Res., 10, 13-34.

Wright, J.V., 1980. Stratigraphy and geology of the welded air-fall tuffs of Pantelleria, Italy. Geol. Rundschau, 69, 263-291.

Wright, J.V., Smith, A.L. and Self, A., 1980. A working terminology of pyroclastic deposits. J. Volcanol. Geotherm. Res., 8, 315-336.

APPENDIX I

TWO EXAMPLE SECTIONS FROM THE BISKUPSFELL FORMATION

SECTION I

This profile is located on the western rim of the main fissure wall (Figs. 1 and 2), and is composed of air-fall ejecta deposited during the second eruption phase, the Hawaiian-Strombolian phase. The total thickness of the section is over 7 m (Fig. 3), the base is not exposed but covered with scree material. The lowermost unit, ranging at least 2.6 m, accumulated during the first Hawaiian eruption cycle. The basal 0.8-0.9 m (layer A) consists of dark grey, agglutinated to partly welded spatter (Fig. 4), with the average maximum diameter of the three largest spatter bombs being 32 cm. Vesicles are abundant. The matrix is fine-grained consisting of microcrystalline plagioclase, opaque glass and some olivine. Plagioclase phenocrysts are rare. The flattening ratio (Fr) of this basal layer is 4 indicating just a slight secondary flattening of the spatter bombs. No lithic fragments are present.

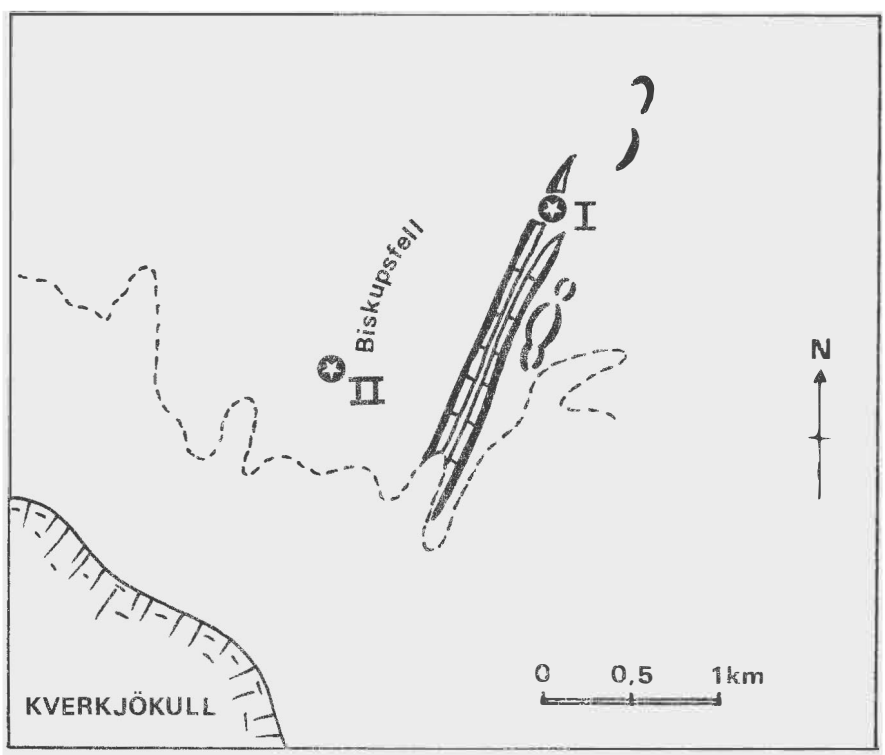

Fig. 1. The locations of the two example sections, I and II. The broken line marks the extent of the glacial moraines.

SW NE

Fig. 2. The north-western rim of the Biskupsfell fissure showing the location of Section I (column).

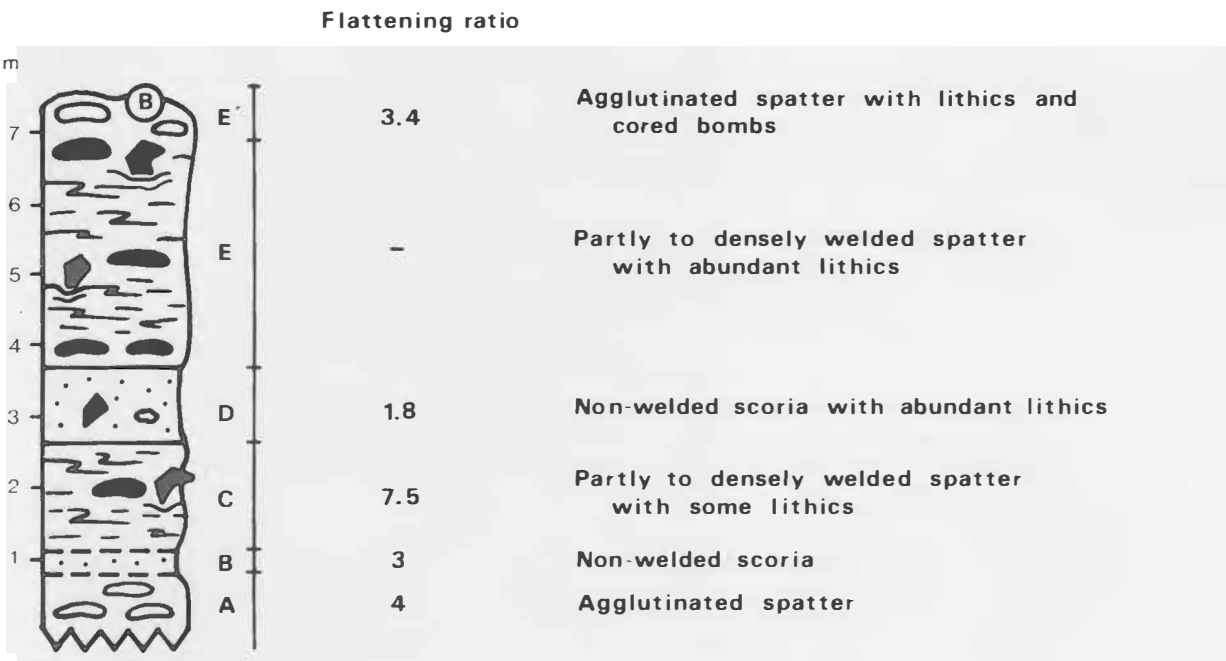

Fig. 3. Stratigraphy of the air-fall ejecta shown in Section I on the north-western rim of the Biskupsfell fissure.

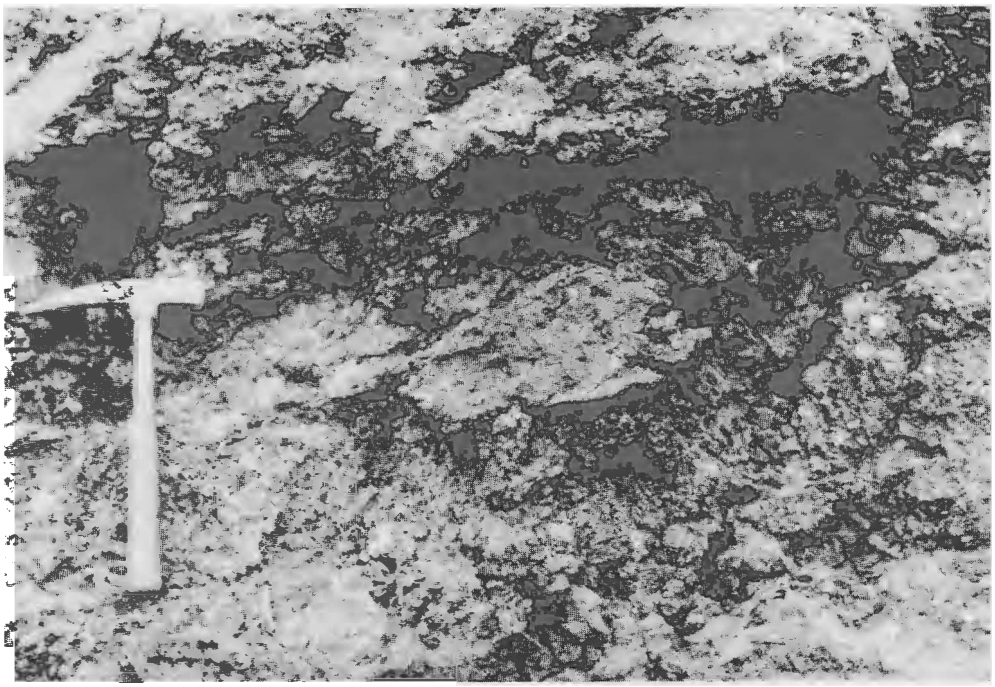

Fig. 4. Layer A, Section I, agglutinated to partly welded spatter.

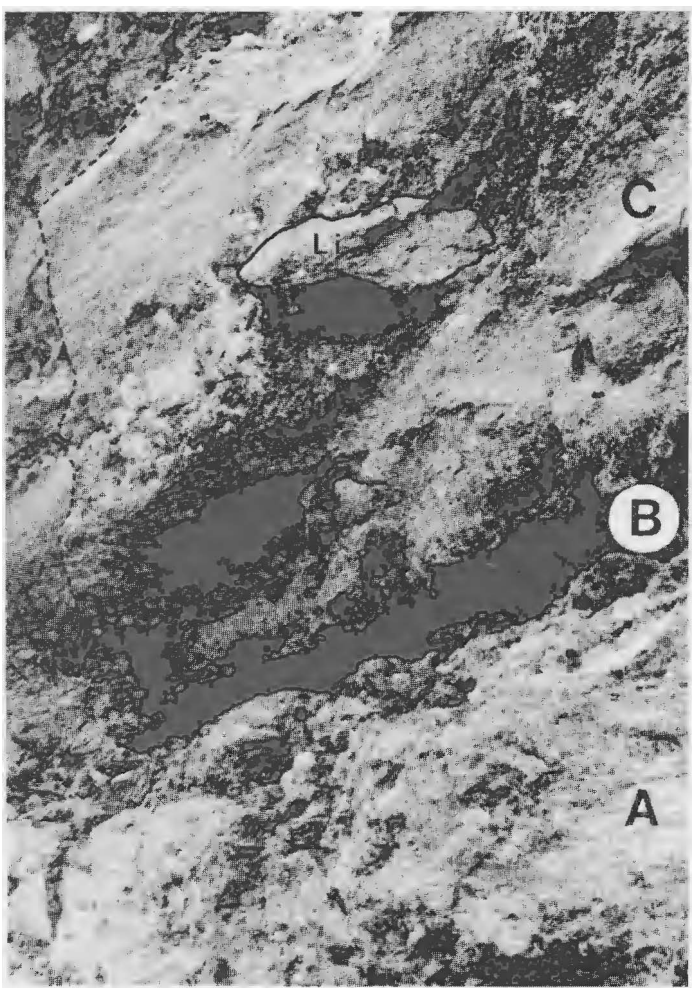

Fig. 5. Layers A-C, Section I. The non-welded scoria, layer B, is partly weathered away. Note the large lithic fragment with its partly welded surroundings in the densely welded C-layer.

A 0.2 m thin, brick-red scoria lens (layer B) breaks off the basal spatter (Fig. 5). The scoria bed consists almost entirely of lapilli-sized, highly vesicular, ragged scoria with some coarser cow-dung bombs and a few small lithics. The scoria is non-welded in the middle of the bed but shows a slight welding towards the lower and upper contacts. Above the scoria lies a dark grey, 1.6 m thick densely welded spatter layer (C) with lenses of partly welded spatter (Fig. 5). Fr-ratio for the partly welded spatter is 7.5, in the densely welded parts the boundaries of the individual spatter clasts have been destroyed due to dense welding. Some lithic fragments are present. They are composed of both fine-grained pillow lava and of porphyritic pillow lava fragments and of sharp-edged fragments of densely welded material. The average maximum diameter of the three largest lithic fragments is 24 cm. The cooling effect of shallowly derived lithics can be seen in Fig. 5, where the immediate neighbourhood of a large lithic is just partly welded in the otherwise densely welded layer.

The heat from the under- and the overlying spatter beds (layers A and C, respectively) have caused a slight, incipient welding effect on the scoria bed between them. The contacts between these three morphologically different beds are somewhat gradational which indicates that they were accumulated in a rapid succession during one eruption phase.

Above the first Hawaiian spatter unit (layers A-C) lies a 1.1 m thick bed of brownish red lapilli scoria (layer D). The contact to the underlying unit is sharp and has been interpreted as due to a change in the eruption mechanism, i.e. from a Hawaiian fire fountaining to a more explosive, Strombolian episode. Possibly a short time interval (some hours) occurred between these two eruptive cycles. The scoria unit is composed of unconsolidated, coarse lapilli with some cow-dung bombs and abundant lithics (Fig. 6). The scoria bombs have a flattening ratio of 1.8, i.e. no secondary flattening occurred after the accumulation. The lithic fragments consist both of pillow lava fragments and of large blocks of welded spatter, derived from the underlying spatter unit. The average maximum diameter of the three largest lithic fragments is 57 cm. Cored bombs are also abundant, having the average maximum diameter of the three largest bombs as 18 cm.

There is a sharp contact to the overlying unit indicating again a change in the eruption mechanism. The uppermost part of Section I (layer E) forms a 4 m thick unit built up during the second Hawaiian fire fountain cycle. The layer E consists of alternating lenses of dark violet-grey, partly welded and dark grey, densely welded spatter. The spatter is made up of large, regular cow-dung bombs, the average maximum diameter of the three largest bombs is 72 cm. The southern part of this unit follows a slight topographic low; here the welded spatter has become rheomorphic and has been partly flown back to the fissure (Fig. 2).

Fig. 6. Layer D, Section I, non-welded scoria with abundant lithic fragments consisting both of dark grey, densely welded material (large fragments) and of pillow lava fragments (arrows).

Fig. 7. Layer E, Section I, partly to densely welded spatter. The large lithic fragment has formed a pronounced bomb sag in the welded spatter.

Lithic fragments are abundant and range sizes larger than in the previous units; large ballistically transported lithics have often formed a pronounced bomb sag on the underlying welded layer (Fig. 7). Lithics consist both of pillow lava fragments and of densely welded spatter blocks. The average maximum size of the three largest lithic fragments is 117 cm. The top of the section, ca. 0.5 m thick layer (E'), is composed of red to brown, agglutinated spatter with a Fr-ratio of 3.4. Some scoriaceous material is also present. Cored bombs are abundant on the top, the average maximum diameter of the three largest bombs is 46 cm.

SECTION II

This section is located on the top of a pillow lava ridge, about 0.8 km W from the main fissure (Fig. 1). On the measured site the contact to the pillow lava is not exposed but in a few places southwards along the ridge a weathered pillow lava surface could be found directly under the basal spatter unit. Chemical analyses concerning this section are represented in Table 2, nos. 4A, 4C, 4D and 4E (p. 53). The thickness of the Section II is about 5 meters (Fig. 8). The basal > 0.7 m (layer A) is composed of dark grey to brown, partly welded spatter with a flattening ratio 9.4 (Fig. 9). The matrix material is very fine-grained consisting mostly of microcrystalline plagioclase needles and of small olivine crystals sub-ophitically intergrown with opaque glass. Some lithic fragments are present, the average maximum size of the three largest lithics being 9 cm.

The layer A passes into a 0.2 m thin, brownish red layer composed of incipiently to partly welded spatter and scoria (layer B). Small lithics, usually 2-4 cm in diameter, are abundant. The average maximum size of the three largest lithics is 7 cm. The Fr-ratio in this bed is 6.2. The average maximum diameter of the three largest spatter bombs is 31 cm.

Above the layer B lies a 1.1 m thick bed (layer C) made up of dark grey, intensively welded spatter (Figs. 9 and 10). The matrix is aphanitic, almost glassy. Some plagioclase phenocrysts are present. The Fr-ratio in the middle of the layer is 18, decreasing both up- and downwards. The spatter shows evidence of rheomorphism; the strongly flattened and stretched spatter grains form a distinct lineation along a horizontal foliation plane (originally caused by the compaction of the spatter bombs during welding). The lineation follows the slope direction, which is here nearly E-W. Lithics, both fine-grained pillow lava and porphyritic pillow lava fragments, are abundant (Fig. 10). The average maximum size of the three largest lithic fragments is 12 cm.

The contacts between these three layers are gradational (see Fig. 9) suggesting that their accumulation occurred in a rapid succession. These layers, A-C, correspond very well with the layers A-C in Section I.

SECTION II

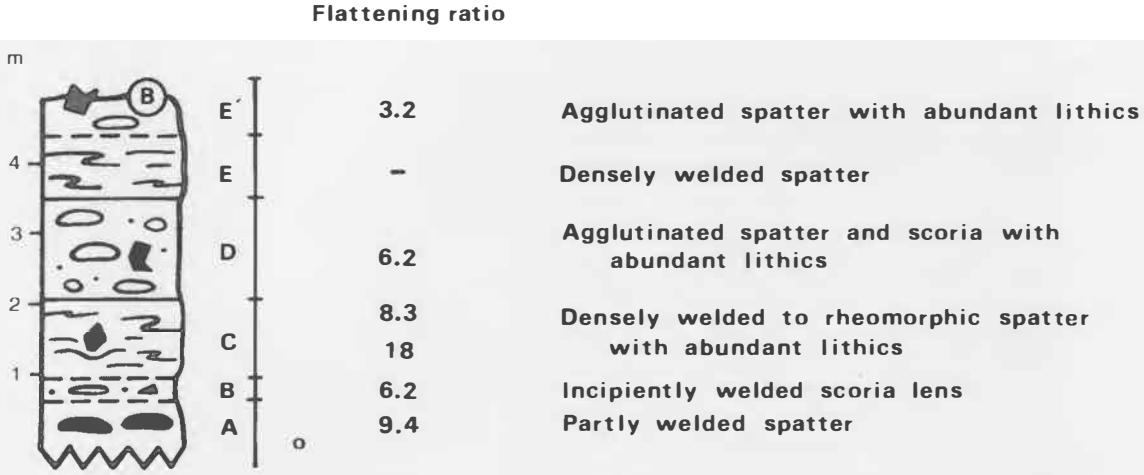

Fig. 8. Stratigraphy of the air-fall ejecta shown in Section II, situated ca 0.7 km W from the Biskupsfell fissure (see Fig. 1).

Fig 9. Layers A-C, Section II, partly welded, incipiently welded and rheomorphic spatter, respectively.

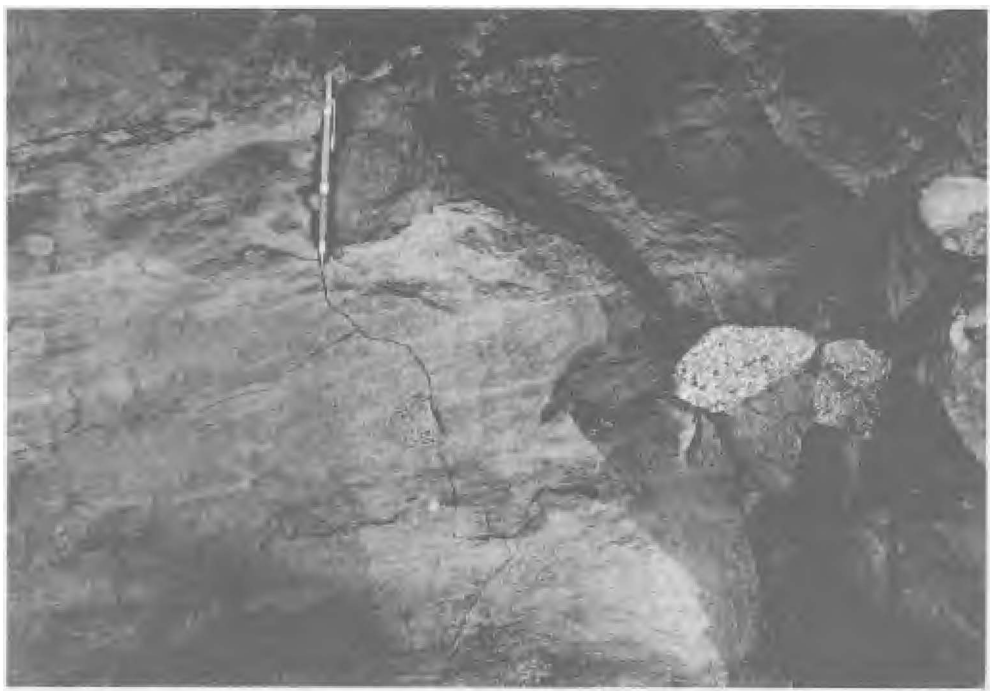

Fig. 10. Layer C, Section II, rheomorphic spatter with flow texture and with abundant lithics.

Fig. 11. Layer D, Section II, agglutinated to incipiently welded spatter and scoria. Some lithic fragments are pointed out with arrows.

A 1.5 m thick layer (D) of red to brownish grey Strombolian scoria and spatter overlies the first Hawaiian unit separated from it by a sharp contact. The material ranges from agglutinated to incipiently and partly welded spatter and scoria (Fig. 11). The flattening ratio in this unit is 6.2. Welding seems to increase upwards as well as the amount of spatter bombs in the proportion to scoria. Lithic fragments of the same type as in the previous unit are abundant, the average maximum size of the three largest lithics is 18 cm. There is again a marked contact to the overlying unit though not as sharp as the lower one.

The uppermost unit is composed of a 0.9 m thick lower part (layer E) and of a 0.4 m thick top layer (E'). The dark grey E-layer is densely welded and shows also evidence of rheomorphism (flow texture). Towards the top this unit passes to partly welded and agglutinated spatter (layer E'). The flattening ratio on the top is 3.2. The spatter bombs are composed of large cow-dung types, occasionally fusiform and bread-crust bombs are present. The average maximum diameter of the three largest spatter bombs is 47 cm. Cored bombs are abundant with the average maximum size of the three largest ones being 35 cm. The average maximum size for the three largest lithic fragments measured on the top layer is 20 cm. Small amounts lapilli-sized scoria is also present.

APPENDIX II

Plagioclase analyses. Microphenocrysts (skeletal plagioclase needles and laths).

Temperature calculations by means of natural glasses.

	SiO2	Al2O3	FeOt	CaO	NaO2	K2O	An%	Temp.C
1b	52.4	31.6	0.98	14.0	3.89	0.11	67.3	1165 C
	53.2	30.7	1.17	13.4	4.33	0.15	64.1	1149 C
	52.8	29.8	1.37	13.2	4.23	0.13	64.7	1152 C
	51.7	29.1	2.27	13.0	4.33	0.16	64.8	1153 C
1c(1)	54.3	28.7	1.04	12.0	4.53	0.15	60.4	1119 C
	54.3	29.0	1.33	12.0	4.89	0.16	59.0	1113 C
(2)	51.7	31.5	0.77	14.2	3.58	0.09	69.2	1165 C
3	51.1	28.1	1.21	11.7	4.22	0.18	61.7	1144 C
	47.2	28.5	1.41	10.9	3.95	0.14	62.2	1146 C

Temperature calculations by means of fused glasses.

4A(1)	56.2	25.8	1.01	9.34	6.42	0.45	45.5	1066 C
(2)	53.1	23.7	1.12	11.1	5.56	0.22	53.7	1103 C
	53.2	24.6	1.13	11.2	5.35	0.27	54.7	1109 C
	52.6	28.1	1.06	11.8	5.18	0.23	56.6	1118 C
(3)	50.9	27.1	0.91	12.9	4.16	0.16	63.8	1153 C
	49.5	27.6	0.77	13.7	3.84	0.10	67.0	1168 C
	51.0	28.1	0.89	13.4	4.61	0.15	62.3	1145 C
	51.8	29.6	0.82	13.6	3.98	0.12	66.0	1163 C
	51.5	29.8	0.97	13.3	4.26	0.17	64.0	1154 C
	50.1	29.6	0.83	13.6	3.73	0.06	67.6	1171 C
	51.1	29.3	1.01	13.2	4.06	0.16	65.0	1159 C
(4)	48.7	28.2	0.74	14.2	3.58	0.13	68.9	1180 C
	49.5	26.6	0.89	14.2	3.60	0.11	69.1	1180 C
	50.3	31.3	0.73	14.8	3.38	0.15	70.9	1191 C
4E(1)	57.5	18.3	1.50	6.75	6.93	0.94	36.7	1034 C
	58.8	22.0	1.10	6.61	5.53	1.44	38.9	1055 C
	57.0	26.2	1.07	8.78	6.62	0.51	43.3	1063 C
(2)	54.9	27.5	1.11	10.6	5.70	0.29	51.7	1102 C
	53.5	27.2	1.10	11.4	5.24	0.25	55.5	1120 C
	53.8	27.8	1.18	11.9	4.80	0.22	58.9	1136 C
	53.5	27.7	1.27	11.8	4.98	0.26	57.8	1131 C
(3)	54.9	28.8	1.17	13.1	3.80	0.29	66.0	1174 C
	48.8	24.3	1.03	14.6	3.16	0.06	72.7	1206 C

plagioclase analyses continued

5C(1)	51.8	30.0	0.84	13.3	3.83	0.06	66.6	1164 C
	51.6	30.4	0.89	13.4	3.65	0.08	67.8	1171 C
	49.4	30.6	0.80	12.6	3.75	0.03	66.0	1161 C
	51.8	30.2	0.80	12.8	3.86	0.13	65.3	1159 C
	52.3	29.8	0.82	13.2	3.93	0.13	65.6	1161 C
(2)	50.3	30.5	0.68	14.2	3.30	0.10	70.7	1188 C
8 (1)	56.5	25.3	1.78	8.95	5.66	0.31	49.4	1053 C
(2)	56.1	28.8	1.49	11.2	4.75	0.20	58.3	1096 C
	56.2	27.3	1.08	10.1	4.88	0.33	54.3	1078 C
	54.3	28.3	1.72	11.1	4.73	0.21	58.5	1097 C
	54.7	29.0	1.09	11.5	4.73	0.14	58.6	1097 C
	53.8	29.0	1.21	12.0	4.35	0.33	61.0	1113 C
9 (1)	54.5	28.3	1.25	11.2	4.75	0.20	58.0	1118 C
(2)	50.9	30.1	0.80	12.3	3.82	0.07	64.9	1150 C
	54.1	30.2	0.79	13.2	3.60	0.13	67.4	1165 C
	50.4	30.7	0.83	14.4	3.28	0.06	71.5	1186 C
14(1)	58.7	21.6	2.45	9.78	5.62	1.05	50.6	1091 C
(2)	54.2	26.3	1.71	10.9	4.97	0.24	56.9	1111 C
	56.2	27.5	1.41	11.2	5.35	0.28	55.2	1103 C
	55.5	28.2	1.09	11.1	4.95	0.18	56.5	1108 C
	52.5	27.2	1.51	10.9	4.77	0.22	57.5	1114 C
	51.7	26.7	1.04	10.9	4.10	0.17	60.6	1128 C
	53.4	25.1	1.41	11.4	4.27	0.17	61.2	1131 C
	53.4	27.6	1.30	12.0	4.76	0.17	59.6	1123 C
	53.8	28.2	1.29	11.4	4.89	0.18	57.7	1114 C

Plagioclase analyses. Phenocrysts.

Temperature calculations by means of natural glasses.

	SiO2	Al2O3	FeOt	CaO	Na2O	K2O	An%	Temp.C
1b	47.5	34.4	0.63	17.7	1.89	0.11	83.6	1274 C
1c	48.9	32.7	0.69	15.4	2.40	0.06	78.3	1220 C
	47.6	33.0	0.67	17.4	1.83	0.07	84.0	1264 C
	48.7	33.5	0.67	16.4	2.23	0.07	80.4	1235 C

Temperature calculations by means of fused glasses.

14	48.6	34.7	0.70	16.5	2.04	0.05	81.9	1253 C
	48.3	33.9	0.56	16.6	1.76	0.10	83.7	1270 C
	48.0	33.7	0.61	16.2	1.96	0.07	82.1	1255 C

Olivine analyses. Microphenocrysts.

Temperature calculations by means of natural glasses.

	SiO2	FeOt	MgO	MnO	CaO	NiO	Fo%	Temp.C
1c	35.5	27.6	34.0	0.46	0.30	0.02	68.7	1079 C
	37.7	27.0	35.6	0.37	0.30	0.06	70.1	1076 C
	37.9	27.3	35.3	0.38	0.31	0.04	69.7	1079 C
	37.4	26.7	32.2	0.35	0.30	0.05	68.2	1092 C

Temperature calculations by means of fused glasses.

4A(a)	37.2	21.9	37.3	1.23	0.31	0.05	75.3	1092 C
	36.6	21.3	37.4	1.10	0.26	0.10	75.8	1089 C
	37.9	20.8	37.3	1.06	0.31	0.06	76.2	1091 C
	38.7	21.4	34.9	1.18	0.32	0.07	74.4	1105 C
(b)	35.0	30.3	30.1	1.51	0.29	0.02	63.9	1139 C
4E(a)	34.6	37.6	23.9	1.89	0.33	0.02	53.1	1210 C
(b)	34.1	42.9	18.4	2.35	0.44	0.05	43.4	1287 C
	34.8	43.2	19.1	2.22	0.61	0.00	44.0	1282 C
9	32.5	47.5	16.8	0.75	0.47	0.01	38.7	1297 C
	33.4	46.3	18.5	0.69	0.34	0.00	41.6	1269 C
15	38.0	23.4	37.7	0.31	0.29	0.09	74.1	1108 C
	38.8	22.0	39.7	0.31	0.26	0.06	76.3	1100 C
	38.1	23.7	38.3	0.26	0.32	0.06	74.3	1107 C
	39.5	21.5	39.9	0.26	0.29	0.10	76.8	1100 C

Olivine analyses. Phenocrysts.

Temperature calculations by means of fused glasses.

	SiO2	FeOt	MgO	MnO	CaO	NiO	Fo%	Temp.C
5C	36.9	26.2	35.0	0.42	0.25	0.01	70.4	1106 C
	37.8	26.2	35.7	0.40	0.24	0.01	70.8	1105 C